Appendix B

B.1. Orthogonal functions

A set of functions are orthogonal to each other when

$$\frac{1}{T}\int_{T} O(i,t)\ O(j,t) = \begin{cases} 1 & for\ \ i = j \\ 0 & for\ \ i \neq j \end{cases} \qquad \textbf{(B. 1)}$$

Some of the non-sinusoidal orthogonal functions are Rademacher functions, Hadamard functions and Walsh functions. These functions are preferred over a set of orthogonal functions derived from sin or cos functions for addressing matrix LCDs. This is because they have only two levels (+1 and −1), hence the hardware realization of drive waveforms becomes simple.

The rectangular block functions are the simplest of orthogonal functions and are derived from diagonal matrix where the amplitudes of all the diagonal elements are same. The line by line addressing techniques uses the rectangular block functions to drive the matrix LCDs. The rectangular block function with its matrix representation is given in Figure B.1-1.

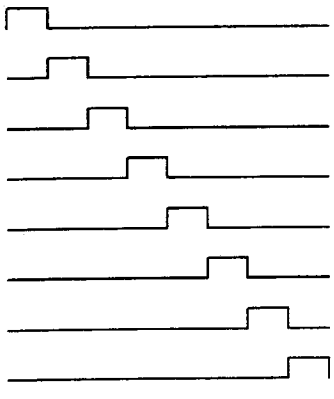

$$\begin{bmatrix} 1 & 0 & 0 & 0 & 0 & 0 & 0 & 0 \\ 0 & 1 & 0 & 0 & 0 & 0 & 0 & 0 \\ 0 & 0 & 1 & 0 & 0 & 0 & 0 & 0 \\ 0 & 0 & 0 & 1 & 0 & 0 & 0 & 0 \\ 0 & 0 & 0 & 0 & 1 & 0 & 0 & 0 \\ 0 & 0 & 0 & 0 & 0 & 1 & 0 & 0 \\ 0 & 0 & 0 & 0 & 0 & 0 & 1 & 0 \\ 0 & 0 & 0 & 0 & 0 & 0 & 0 & 1 \end{bmatrix}$$

Figure B.1-1 Rectangular block function and its matrix representation

The Rademacher functions are square waveforms with frequencies decreasing (or increasing) successively by factors of two. The Rademacher functions are easy to generate,

they are just the output of a binary counter. That is from a n-bit counter one can generate n-Rademacher functions having 2^n time intervals. The first four of Rademacher functions is shown in Figure B.1-2. The first function is equal to +1 for the entire time interval. The Rademacher functions can be used to generate other orthogonal functions such as Hadamard and Walsh functions [74].

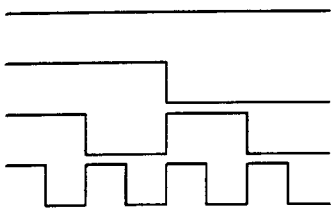

$$\begin{bmatrix} +1 & +1 & +1 & +1 & +1 & +1 & +1 & +1 \\ +1 & +1 & +1 & +1 & -1 & -1 & -1 & -1 \\ +1 & +1 & -1 & -1 & +1 & +1 & -1 & -1 \\ +1 & -1 & +1 & -1 & +1 & -1 & +1 & -1 \end{bmatrix}$$

Figure B.1-2 Rademacher function and its matrix representation.

The Hadamard matrices are easy to generate, the lowest-order Hadamard matrix is of the order one and two are defined as

$$H_1 = [+1]$$

and

$$H_2 = \begin{bmatrix} +1 & +1 \\ +1 & -1 \end{bmatrix}$$

The higher order Hadamard matrices are obtained from the recursive relationship called Kronecker product and is given by

$$H_N = H_{\frac{N}{2}} \otimes H_2 = \begin{bmatrix} H_{\frac{N}{2}} & H_{\frac{N}{2}} \\ H_{\frac{N}{2}} & -H_{\frac{N}{2}} \end{bmatrix} \qquad \text{(B. 2)}$$

Where, $\otimes$ denotes the Kronecker product.

For example the Hadamard matrix of order four (H_4) is given by

$$H_4 = H_{4/2} \otimes H_2 \qquad \text{(B. 3)}$$

$$H_4 = H_2 \otimes H_2$$

they are just the output of a binary counter. That is from a n-bit counter one can generate n-Rademacher functions having 2^n time intervals. The first four of Rademacher functions is shown in Figure B.1-2. The first function is equal to +1 for the entire time interval. The Rademacher functions can be used to generate other orthogonal functions such as Hadamard and Walsh functions [74].

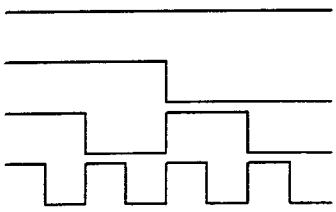

$$\begin{bmatrix} +1 & +1 & +1 & +1 & +1 & +1 & +1 & +1 \\ +1 & +1 & +1 & +1 & -1 & -1 & -1 & -1 \\ +1 & +1 & -1 & -1 & +1 & +1 & -1 & -1 \\ +1 & -1 & +1 & -1 & +1 & -1 & +1 & -1 \end{bmatrix}$$

Figure B.1-2 Rademacher function and its matrix representation.

The Hadamard matrices are easy to generate, the lowest-order Hadamard matrix is of the order one and two are defined as

$$H_1 = [+1]$$

and

$$H_2 = \begin{bmatrix} +1 & +1 \\ +1 & -1 \end{bmatrix}$$

The higher order Hadamard matrices are obtained from the recursive relationship called Kronecker product and is given by

$$H_N = H_{\frac{N}{2}} \otimes H_2 = \begin{bmatrix} H_{\frac{N}{2}} & H_{\frac{N}{2}} \\ H_{\frac{N}{2}} & -H_{\frac{N}{2}} \end{bmatrix} \qquad \textbf{(B. 2)}$$

Where, $\otimes$ denotes the Kronecker product.

For example the Hadamard matrix of order four (H_4) is given by

$$H_4 = H_{4/2} \otimes H_2 \qquad \textbf{(B. 3)}$$

$$H_4 = H_2 \otimes H_2$$

$$H_4 = \begin{bmatrix} H_2 & H_2 \\ H_2 & -H_2 \end{bmatrix} \tag{B. 4}$$

$$H_4 = \begin{bmatrix} +1 & +1 & +1 & +1 \\ +1 & -1 & +1 & -1 \\ +1 & +1 & -1 & -1 \\ +1 & -1 & -1 & +1 \end{bmatrix} \tag{B. 5}$$

Similarly the Hadamard matrix of order 8 as shown in Figure B.1-3, from equation (B. 3),

$$H_8 = H_4 \otimes H_2 \tag{B. 6}$$

$$H_8 = \begin{bmatrix} H_4 & H_4 \\ H_4 & -H_4 \end{bmatrix}$$

$$H_8 = \begin{bmatrix} +1 & +1 & +1 & +1 & +1 & +1 & +1 & +1 \\ +1 & -1 & +1 & -1 & +1 & -1 & +1 & -1 \\ +1 & +1 & -1 & -1 & +1 & +1 & -1 & -1 \\ +1 & -1 & -1 & +1 & +1 & -1 & -1 & +1 \\ +1 & +1 & +1 & +1 & -1 & -1 & -1 & -1 \\ +1 & -1 & +1 & -1 & -1 & +1 & -1 & +1 \\ +1 & +1 & -1 & -1 & -1 & -1 & +1 & +1 \\ +1 & -1 & -1 & +1 & -1 & +1 & +1 & -1 \end{bmatrix}$$

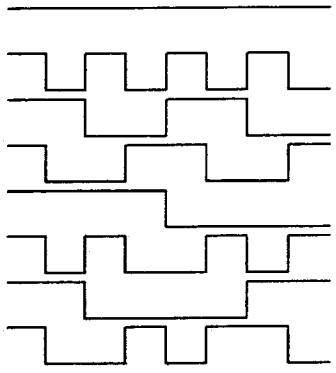

Figure B.1-3 Hadamard matrix of order 8 and its corresponding waveforms.

The matrix shown in equation B.7 below is called Hadamard matrix type 2 of order 4. Where the diagonal elements being −1 while the rest of the elements are +1.

$$H_4 = \begin{bmatrix} -1 & +1 & +1 & +1 \\ +1 & -1 & +1 & +1 \\ +1 & +1 & -1 & +1 \\ +1 & +1 & +1 & -1 \end{bmatrix} \tag{B. 7}$$

Walsh functions can be obtained by rearranging a few rows or columns of the Hadamard matrices. Walsh functions can also generated from the Rademacher functions using Ex-OR (modulo 2 arithmetic) operations called Harmuth's array generator [74]. The Walsh matrix of order 8 and its corresponding waveforms are shown in Figure B.1-4.

$$W_8 = \begin{bmatrix} +1 & +1 & +1 & +1 & +1 & +1 & +1 & +1 \\ +1 & +1 & +1 & +1 & -1 & -1 & -1 & -1 \\ +1 & +1 & -1 & -1 & -1 & -1 & +1 & +1 \\ +1 & +1 & -1 & -1 & +1 & +1 & -1 & -1 \\ +1 & -1 & -1 & +1 & +1 & -1 & -1 & +1 \\ +1 & -1 & -1 & +1 & -1 & +1 & +1 & -1 \\ +1 & -1 & +1 & -1 & -1 & +1 & -1 & +1 \\ +1 & -1 & +1 & -1 & +1 & -1 & +1 & -1 \end{bmatrix}$$

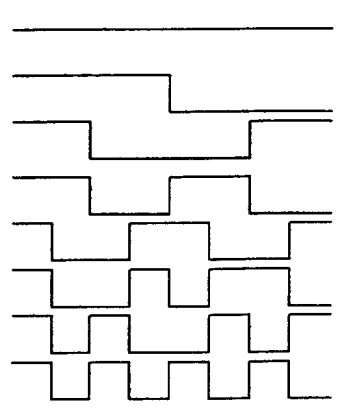

Figure B.1-4 Walsh matrix of order 8 and its corresponding waveforms.

Apart from Walsh functions and Hadamard matrices, the row select patterns generated from Pseudo Random Binary Sequence (PRBS) is a good choice for row waveforms. Because the number of transitions in a PRBS and its shifted waveforms is either 2^{s-1} or $2^{s-1}+2$. Where, s is the number of flip-flops necessary in the shift register circuit used for generating the sequence. This difference is not much for a very long sequence and in any case less than that of Hadamard or Walsh functions. That is number of transitions in Hadamard and Walsh functions ranges from 0 to 2^s-1 as seen in Figure B.1-3 and Figure B.1-4, respectively. For example, Figure B.1-5 shows the PRBS waveform generated by three bit shift register.

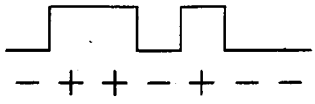

Figure B.1-5 Pseudo random binary sequence of length seven generated using three bit shift register.

Figure B.1-6 shows the 7x7 PRBS matrix and its equivalent waveforms formed by shifting the sequence shown in Figure B.1-5. The frequency spectrum of these waveforms are same and they are identical except for the shift in time domain, but this is not orthogonal. Hence, they are not suitable for driving matrix LCDs. However these sequence can be converted to orthogonal form by adding a column of +1 to the matrix as shown in the Figure B.1-7.

$$P_7 = \begin{bmatrix} -1 & +1 & +1 & -1 & +1 & -1 & -1 \\ +1 & +1 & -1 & +1 & -1 & -1 & -1 \\ +1 & -1 & +1 & -1 & -1 & -1 & +1 \\ -1 & +1 & -1 & -1 & -1 & +1 & +1 \\ +1 & -1 & -1 & -1 & +1 & +1 & -1 \\ -1 & -1 & -1 & +1 & +1 & -1 & +1 \\ -1 & -1 & +1 & +1 & -1 & +1 & -1 \end{bmatrix}$$

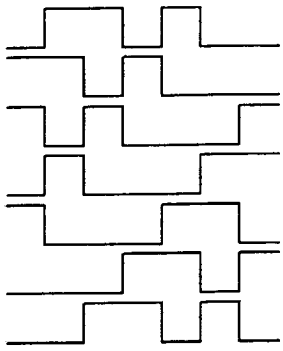

Figure B.1-6 PRBS matrix generated using the sequence shown in Figure B-6 and its corresponding waveforms which are not orthogonal.

$$P_8 = \begin{bmatrix} +1 & -1 & +1 & +1 & -1 & +1 & -1 & -1 \\ +1 & +1 & +1 & -1 & +1 & -1 & -1 & -1 \\ +1 & +1 & -1 & +1 & -1 & -1 & -1 & +1 \\ +1 & -1 & +1 & -1 & -1 & -1 & +1 & +1 \\ +1 & +1 & -1 & -1 & -1 & +1 & +1 & -1 \\ +1 & -1 & -1 & -1 & +1 & +1 & -1 & +1 \\ +1 & -1 & -1 & +1 & +1 & -1 & +1 & -1 \end{bmatrix}$$

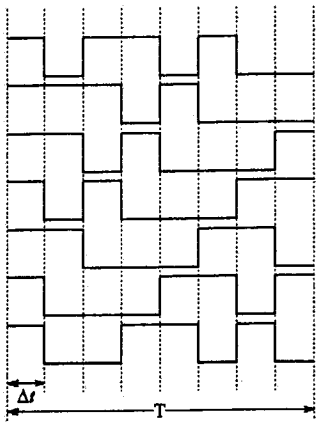

Figure B.1-7 PRBS matrix and its corresponding waveforms which is orthogonal to each other.

The elements of Walsh, Hadamard and PRBS matrices are either +1 or −1. The elements of these matrices can be represented as $O(i, j)$, where i and j corresponds to row and column of the orthogonal matrix. The columns of the matrix are corresponds to a time axis consists of q equal time intervals (Δt) over the period T as shown in the Figure B.1-7. The columns of these orthogonal matrices are used as row select patterns. The orthogonality condition given in equation (B.1) can be expressed in discrete form as

$$\frac{1}{q}\sum_{t=1}^{q} O(i,t)O(j,t) = \begin{cases} 1 & i = j \\ 0 & i \neq j \end{cases} \qquad \textbf{(B. 8)}$$

Appendix C

C.1. Electro-optic measurements

The typical single pixel electro-optic measurement setup for normal incidence light is as shown in the Figure C.1-1. The liquid crystal test cell is placed between the two polarizers. The two polarizers can be rotated to fix the direction of the polarizing direction with reference to the liquid crystal cell. The polarizing axis is parallel to the rubbing direction in the respective sides of the test cell to get the measurement in normally white mode configuration. Similarly, if the polralizers are kept parallel to the one of the rubbing direction of the test cell, then it will be in the normally black mode. The waveforms are generated using a computer controlled waveform generator *WFG 500*. The *Hamamatsu* make photodiode G-1957 is used to measure the transmittance light intensity across the cell. The applied *rms* voltage to the cell and the resultant light transmittance from the photodiode is measured using the *hp* 3467A logging multimeter. The entire optical setup is mounted on the optical bench as shown in the Figure C.1-1.

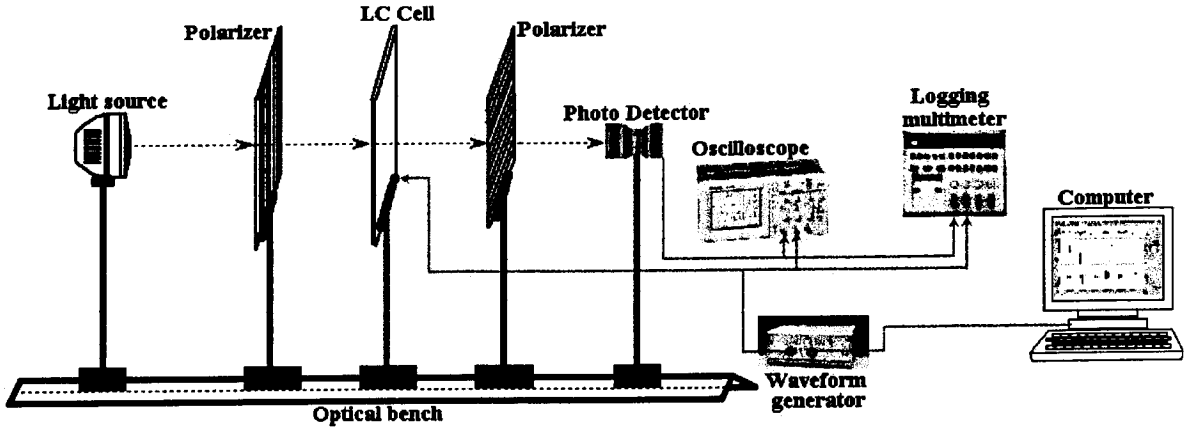

Figure C.1-1 Single pixel electro-optic setup to measure the transmission across the liquid crystal cell.

The waveform generator *WFG-500* has eight channels and a common time base. The minimum pulse width is 200ns and the maximum amplitude is ±100volts. The resolutions are 100ns and 50mV, respectively. The generator is controlled by a standard serial interface RS232 port. The row and column waveforms are generated using *MATLAB*® and *C*-programs. The typical row, column and the resultant waveform across the OFF and ON

pixels generated using *WFG*-500 is as shown in the Figure C.1-2(a) and Figure C.1-2(b), respectively.

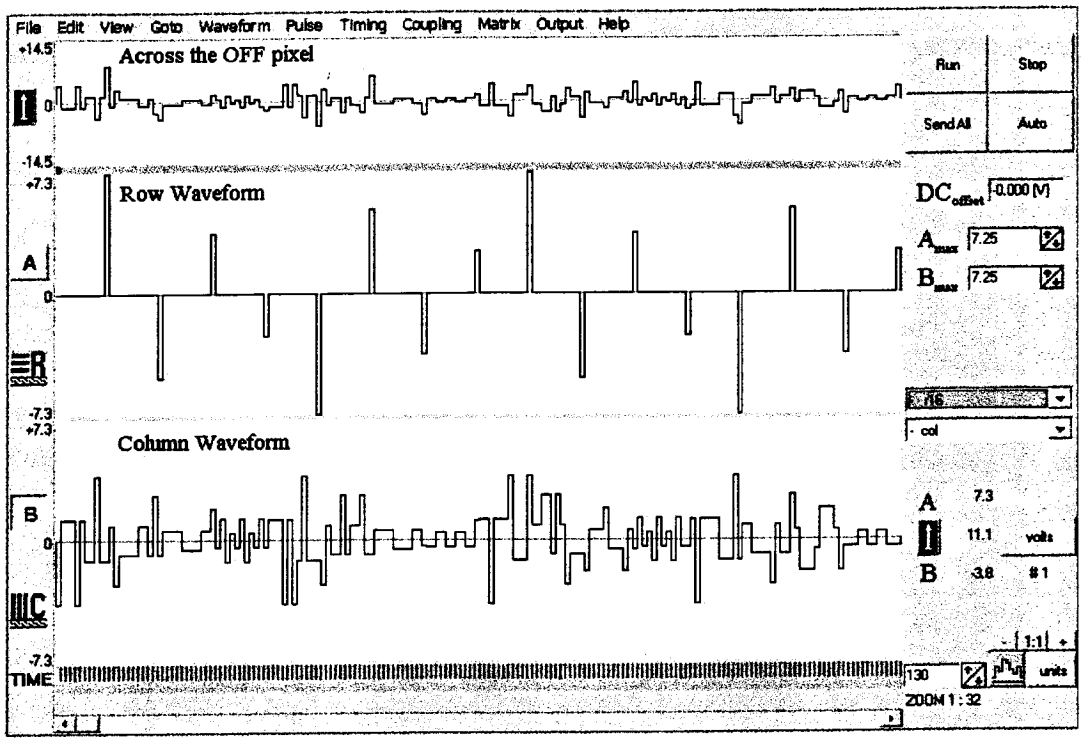

(a)

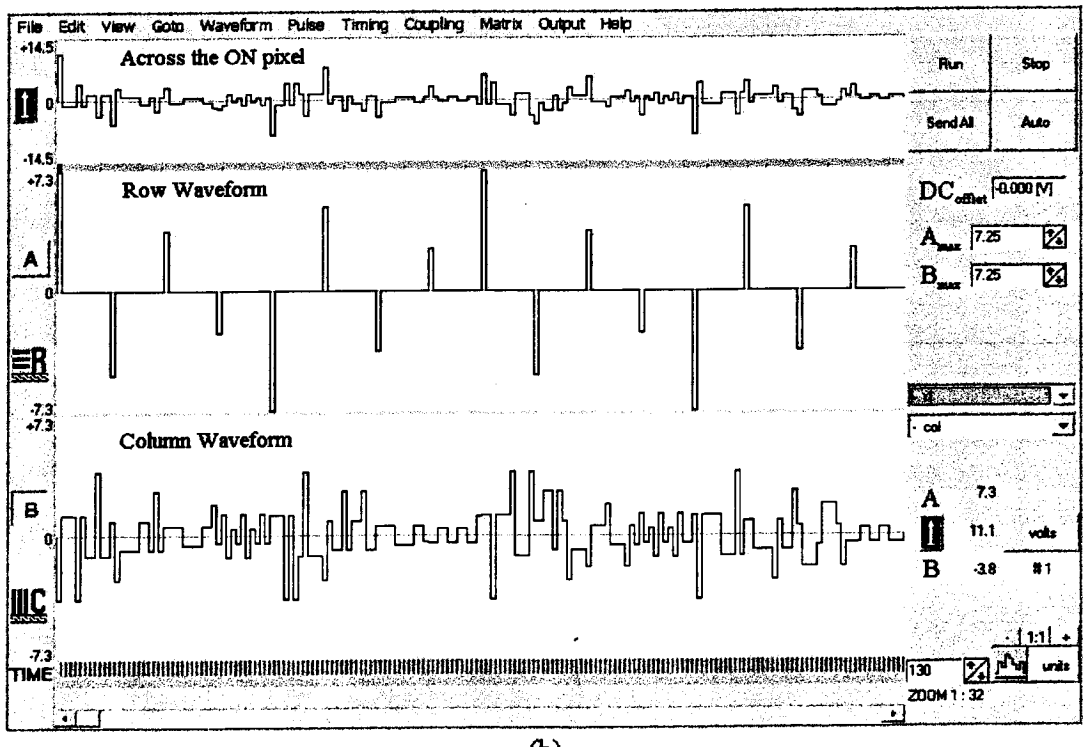

(b)

Figure C.1-2 Generated waveforms using WFG-500 (a) OFF pixel and (b) ON pixel using successive approximation approach based on MLA for a 32x32 matrix LCD by selecting 3 rows at a time.

The typical electro-optic characteristics of the TN LCD for liquid crystal mixture Roche TN 3570 is measured and shown in Figure C.1-3. The threshold voltage (V_{th}), saturation voltage (V_{sat}), sharpness parameter (γ) and the response time, which are discussed in the Appendix A are measured using single pixel electro-optic setup and tabulated in the Table C.1-1.

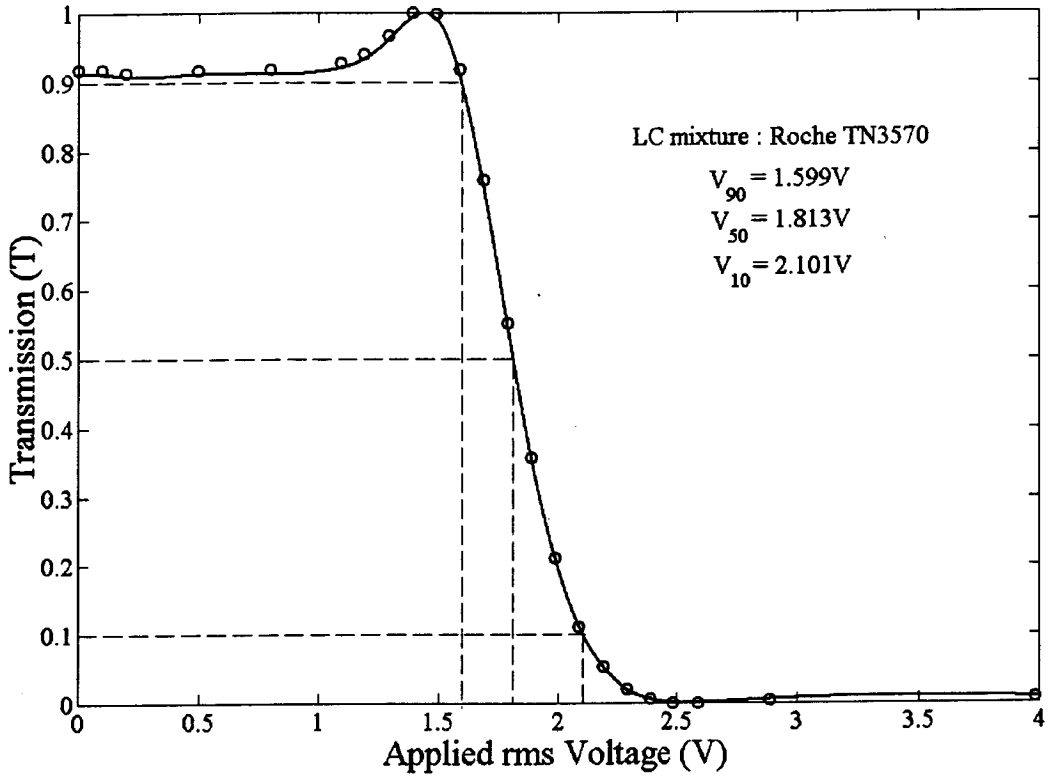

Figure C.1-3 Electro-optic characteristics of the TN LCD (normally white mode) for liquid crystal mixture Roche TN3570.

While multiplexing 32 rows matrix LCD, the selection ratio is 1.1956. The rms voltage across the OFF pixels is biased to the threshold voltage (V_{th}). The maximum voltage ratio between the V_{sat} to V_{th} for the liquid crystal mixture used is $\left(\frac{V_{sat}}{V_{th}}\right) = 1.3139$, which is higher than 1.1956. That is electro-optic curve is not steep enough to multiplex 32 rows to give maximum contrast. Hence, with this liquid crystal mixture transmission across the ON pixel is only 68%. Hence, the contrast ratio is lower while using this liquid crystal mixture for multiplexing 32 rows, but it is adequate to demonstrate the technique.

Table C.1-1

Parameter	Measured	Remarks
V_{th}	1.599V	Threshold voltage (V_{th}): rms voltage at which light transmission has changed 10% of the maximum value.
V_{sat}	2.101V	Saturation voltage (V_{sat}): rms voltage at which light transmission has changed 90% of the maximum value.
V_{50}	1.813V	rms voltage at which light transmission has changed 50% of the maximum value.
$\frac{V_{sat}}{V_{th}}$	1.3139	Selection ratio
γ	13.3834	Sharpness parameter, $\gamma = \frac{V_{50} - V_{10}}{V_{10}} 100$
τ_r	26ms	Rise time : Time interval during which the transmission changes from 10% to 90% (Non multiplexed condition, refer Figure A.14, in Appendix A)
τ_f	32ms	Fall time : Time interval during which the transmission changes from 90% to 10%. (Non multiplexed condition, refer Figure C.4)
τ_r	83ms	Rise time : Time interval during which the transmission changes from 10% to 90%. Under multiplexed condition ($N = 32$),refer Figure C.5
τ_f	90ms	Fall time : Time interval during which the transmission changes from 90% to 10%. Under multiplexed condition ($N = 32$), refer Figure C.5

Figure C.1-4 shows the response of the cell for the case of single pixel (i.e., static drive) non-multiplexed condition when square waveform is applied. Here, the applied rms voltage is very much larger than the threshold voltage (V_{th}). The rms voltage across the cell is turned ON and OFF using the computer control. The response of the liquid crystal cell is captured using TDS 220 oscilloscope. The switching time between OFF to ON state is 48ms and from ON to OFF state is around 50ms. The response time is characterised to three constants, the delay time (τ_{dr} and τ_{df}), the rise time (τ_r) and the fall time (τ_f) (see Appendix A, Figure A.14). The measured values from the Figure C.1-4 are tabulated in the following Table C.1-2.

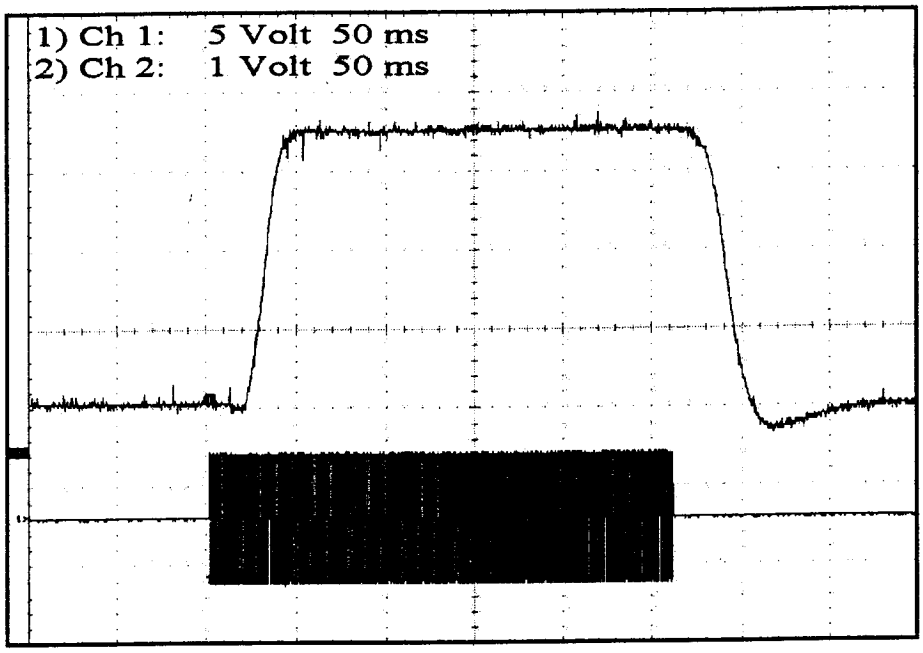

Figure C.1-4 Typical response of an liquid crystal cell for non multiplexed condition.

Table C.1-2

The delay time from the start of the pulse trains to the transmission reaches 10% of the final value	τ_{dr}	22ms
The rise time	τ_r	26ms
The delay time between final value of the transmission to the 90% transmission after the turning off the applied signal.	τ_{df}	18ms
The fall time	τ_f	32ms

In multiplexed condition the switching time is measured. Here, the rms voltage at the time of OFF state is maintained at the threshold voltage (i.e.,1.599volts) of the liquid crystal mixture used. For the case of multiplexing 32 rows the rms voltage across 1.912volts (i.e., Selection ratio times the threshold voltage) is applied to switch the cell to ON state. The typical switching characteristic of the liquid crystal cell under multiplexed condition is shown in the Figure C.1-5. In this case the transmission drops to 68% as compared to the non-multiplexed condition. The switching time measured between OFF to ON is 83ms and from ON to OFF state is around 90ms.

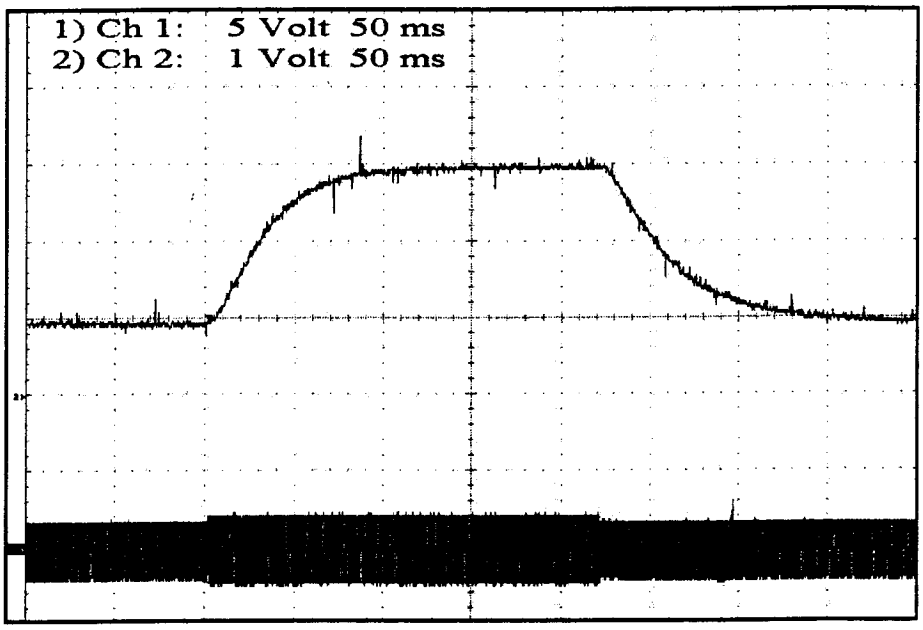

Figure C.1-5 Typical response of a liquid crystal cell under multiplexed condition (i.e., $N = 32$).

References:

1. Burton W Marks, "Power Reduction In Liquid-Crystal Display Modules", IEEE transactions on electron devices, Vol. ED-29, NO.12, pp 1884-1886, (1982).
2. L A Goodman, "Liquid Crystal Displays–Electro-Optic Effects And Addressing Techniques", RCA Review, Vol. 35, pp 613-651, (1974).
3. Allan R Kmetz, "Liquid Crystal Display Prospects In Perspective", IEEE Conference Record of 1972 conference on display devices, pp 119-126, (1972).
4. Alt P M and Pleshko P, "Scanning Limitations Of Liquid Crystal Displays", IEEE Trans. Electron Devices, ED-21, pp 146-155, (1974).
5. Allan R Kmetz and J Nehring, "Ultimate Limits For RMS Matrix Addressing", Proceedings of the Symposium on the Physics and Chemistry of Liquid Crystal Devices (1979), The IBM Research Symposia Series, The physics and chemistry of liquid crystal devices, pp 105-114, (1979).
6. H Kawakami, Y Nagae and E. Kaneko, "Matrix Addressing Technology Of Twisted Nematic Liquid Crystal Display", Conference record of 1976 BIENNIAL Display Conference, pp 50-53, (1976).
7. T N Ruckmongathan, P H Verheggen, T L Welzen, "Reduction Of Brightness Non-Uniformity In Rms Responding Matrix Displays", The International Display Research Conference'90, pp 290-294, (1990).
8. Paolo Maltese, "Complex Polarity Sequences For Directly Driven Liquid Crystal Matrices", Euro Display'87, pp 139-143, (1987).
9. Hiroaki Ideno, Kenji Horikiri and Hirotsugu Arai, "New Driving Method Applied To Large Area Dot Matrix LCDs", Japan Display'83, The 3rd International Display Research Conference (IDRC), PD5, (1983).
10. Y Kaneko, M Haraguchi, H Murakami, H Yamguchi, "Crosstalk-Free Driving Methods For STN-LCDs", SID'90 Digest, pp 412-415, (1990).
11. M Watanabe, Y Inoue, T Ohaba, K Taniguchi, "High Resolution, Large Diagonal Color STN For The Desktop Monitor Applications", International Display Research Conference (IDRC), M–81-87, (1997).
12. I Washizuka, A Sakamoto, "Driving Method To Reduce Shadowing For STN-LCD Module", International Display Workshop'97 (IDW'97), pp 297-300, (1997).

13. Y Kudo, H Mano, S Endo, T Inuzuka, "Enhanced High Addressing-Drive For High Performace STN-LCD", International Display Workshop (IDW'97), pp 257-260, (1997).
14. S Nishitani, H Mano, Y Kudou, T Futami and T Inuzuka, "New Drive Method To Eliminate Crosstalk In STN-LCDs", SID'93 Digest, pp 97-100, (1993).
15. Susumu Kondo, Tomiaki Yamamoto, Akio Murayama, Hitoshi Hatoh and Shoichi Matsumoto, "A Fast-Response Black And White STN-LCD With A Retardation Film", SID'91 Digest, pp 747-750, (1991).
16. T N Ruckmongathan and N V Madhusudana, "New Addressing Techniques For Multiplexed Liquid Crystal Displays", Proceedings of the SID, Vol.24, No.3, pp 259-262, (1983).
17. T N Ruckmongathan, "Some New Addressing Techniques For RMS Responding LCDs", a thesis submitted to Department of Electrical Communication Engineering, Indian Institute of Science, Bangalore, India (1988).
18. T N Ruckmongathan, "A Generalized Addressing Technique For RMS Responding Matrix LCDs", 1988–International Display Research Conference, pp 80-85, (1988).
19. T N Ruckmongathan, "An Addressing Technique With Reduced Hardware Complexity", SID 94 Digest, pp 65-68, (1994).
20. T N Ruckmongathan, "Novel Addressing Methods For Fast Responding LCDs", Reports Res. Lab. Asahi Glass Co. Ltd., Vol. 43 [1], pp 65-87, (1993).
21. B Clifton, D Prince, B Leybold, T J Scheffer, A R Conner and B Greenberg, "Optimum Row Functions And Algorithms For Active Addressing", SID'93 Digest, pp 89-92, (1993).
22. T N Ruckmongathan, T Kuwata, T Ohnishi, S Ihara, H Koh and Y Nakagawa, "A New Addressing Technique For Fast Responding STN LCDs", Japan Display '92, pp 65-68, (1992).
23. T J Scheffer and B Clifton, "Active Addressing Method For High-Contrast Video-Rate STN Displays", SID Intl Symp Digest Tech Papers, pp 228-231, (1992).
24. Peter Pleshko, "Halftone Gray Scale For Matrix-Addressed Displays", Information Display, pp 10-11, October-90, (1990).
25. Kalluri R Sarma, Henry Franklin, Mike Johnson, Keith Frost, Anthony Bernot, "Active Matrix Lcds Using Gray-Scale In Halftone Methods", SID'89 Digest, pp 148-150, (1989).

26. Hideaki Kawakami, Hisao Hanmura and Eiji Kaneko, "Brightness Uniformity In Liquid Crystal Displays", SID'80 Digest, pp 28-29, (1980).
27. Yoshio Suzuki, Mitsunobu Sekiya, Kunihiko Arai and Akio Ohkoshi, "A Liquid-Crystal Image Display", SID'83 Digest, pp 32-33, (1983).
28. T N Ruckmongathan, "Addressing Technique For RMS Responding LCDs – A Review", Proc. of Japan Display'92, pp 77-80, (1992).
29. A R Conner and T J Scheffer, "Pulse-Height Modulation (PHM) Gray Shading Methods for Passive Matrix LCDs", Proc. of Japan Display'92, pp 69-72, (1992).
30. T Otani, K Kumagawa, K Nakanishi, M Matsunami, Y Fukui, T Matsumoto, "Investigation of the Active Drive Method for STN-LCDs", SID'95 Digest, pp 343-346, (1995).
31. Y Hirai, A Nakazawa, K Kawaguchi, H Motegi, H Koh, T Kuwata, Y Nakagawa, T Ohbiki, M Noguchi and H Araki, "A Color STN-LCD for Video Display Using Amplitude-Modulation MLS Technology", SID'95 Digest, pp 339-342, (1995).
32. H Mano, S Nishitani K Kondo, J Taguchi and H Kawakami, "An Eight-Gray-Level Drive Method for Fast-Responding STN-LCDs", SID'93 Digest, pp 93-96, (1993).
33. Ian A Shanks, Paul A Holland and Anthony J Hughes, "Liquid Crystal Oscilloscope Displays", SID'78 Digest, pp 98-99, (1978).
34. Ian A Shanks and Paul A Holland, "Addressing Methods For Non-Multiplexed Liquid Crystal Oscilloscope Displays", SID'79 Digest, pp 112-113, (1979).
35. E Kaneko, "Liquid-Crystal Matrix Displays", Advances in Image Pickup and Displays, Vol. 4, Academic press, Inc. pp 2-87, (1981).
36. T N Ruckmongathan, "An LCD For Multitrace Oscilloscope", SID'86 Digest, pp 128-131, (1986).
37. T N Ruckmongathan, "Flicker-Free Restricted-Pattern Addressing Techniques with Low Supply Voltage", SID'96 Digest, pp 562-565, (1996).
38. Theodorus L Welzen, Adrianus J S M De Vaan, "Low Driving Voltage Display Device", US Patent 4,783,653, Nov. 8, (1988).
39. Karel E Kuijk, Alex V Henzen, Reinder Smid, "Minimum-Voltage Driving of STN LCDs by Optimized Multiple-Row Addressing", Proceedings of Eurodisplay, pp 77-80,(1999).
40. Karel E Kuijk, "Minimum-Voltage Driving of Small STN-LCDs by Optimized Multiple-Row Addressing", Journal of the SID, Vol. 8, Number 2, pp 147-153, (2000).

41. S Chandrasekhar, B K Sadashiva and K A Suresh, "Liquid Crystals Of Disc-Like Molecules", Pramana, Vol. 9, Number 5, pp 471-480, (1977).
42. T Niori, T Sekine, J Watanabe, T Furukawa and H Takezoe, "Distinct Ferroelectric Smectic Liquid Crystals Consisting Of Banana Shaped Achiral Molecules", Journal of Material Chemistry, 6(7), pp 1231-1233, (1996).
43. Ian A Shanks, "The Physics And Display Applications Of Liquid Crystals", Contemp. Phys., Vol. 23, Number 1, pp 65-91, (1982).
44. M Schadt and W Helfrich, " Voltage – Dependent Optical Activity Of A Twisted Nematic Liquid Crystal", Applied Physics Letters, Vol. 18, Number 4, pp 127-128, (1971).
45. T J Scheffer and N Nehring, "A New Highly Multiplexed Liquid Crystal Display", Applied Physics Letters, Vol. 45, Number 10, pp 1021-1023, (1984).
46. G H Heilmeier and L A Zanoni, "Guest-Host Interactions In Nematic Liquid Crystals, A New Electro-Optic Effect", Applied Physics Letters, Vol. 13, Number 3, pp 91-92, (1968).
47. T Uchida and M Wada, "Guest–Host Type Liquid Crystal Displays", Molecular Crystal Liquid Crystal, Vol. 63, pp 19-44, (1981).
48. H Hirai, Y Kinoshita, K Shohara, A Murayama, H Hatoh, S Matsumoto, "Optimisatio Of Cell Condition And Driving Method In A VAN LCD For Color Video Display", Japan Display'89, pp 184-187, (1989).
49. K Ohmuro, S Kataoka, T Sasaki and Y Koike, "Development Of Super-High-Image-Quality Vertical-Alignment-Mode LCD", Society for Information Display'97 Digest, pp 845-848, (1997).
50. H Yoshida, Y Tasaka, H Chida, Y Koike and K Okamoto, "Dual-domain Vertically Aligned TFT-LCD Developed By Irradiation With Unpolarized UV Light From A Tube-Type Light Source", SID'02 Digest, pp 758-761, (2002).
51. R Kiefer, B Weber, F Windsceid and G Baur, "In-Plane Switching of Nematic Liquid Crystals", Japan Display'92, pp 547-550, (1992).
52. M Oh-e, M Ohta, S Aratani, K Kondo, "Principles And Characteristics Of Electro-Optical Behaviour With In-Plane Switching Mode", Asia Display'95, pp 577-580, (1995).

53. Y Mishima, T Nakayama, N Suzuki, M Ohta, S Endoh and Y Iwakabe and H Kagawa, "Development Of A 19-In.-Diagonal UXGA Super TFT-LCM Applied With Super-IPS Technology", Society for Information Display Digest, pp 260-263, (2000).
54. D W Berreman and W R Heffner, "New Bistable Liquid-Crystal Twist Cell", Journal of Applied Physics, Vol. 52, Number 4, pp 3032-3039, (1981).
55. T Tanaka, Y Sato, A Inoue, Y Momose, H Nomura and S Lino, "A Bistable Twisted Nematic (BTN) LCD Driven By A Passive-Matrix Addressing", Asia Display'95, pp 259-262, (1995).
56. Xiao-Yang Huang and Asad Khan, "Reflective Cholesteric Display Technology And Its Application", Proceedings of the 7th Asian Symposium on Information Display (ASID'02), pp 25–28, (2002).
57. G B Bryan-Brown, C V Brown, J C Jones, E L Wood, I C Sage, P Breet and J Rudin, "Grating Aligned Bistable Nematic Device", Proceedings of SID XXVIII, pp 37-40, (1997).
58. J C Jones, E L Wood, G P Bryan-Brown and C V Hui, "Novel Configuration Of The Zenithal Bistable Nematic Liquid Crystal Device", Society for Information Display'98 Digest, pp 858-861, (1998).
59. J C Jones, S M Beldon and E L Wood, "Greyscale in Zenithal Bistable LCD: The route to ultra-low power colour displays", Proceedings of the 7th Asian Symposium on Information Displays, pp 205-208, (2002).
60. Noel A Clark and S T Lagerwall, "Submicrosecond Bistable Electro-Optic Switching In Liquid Crystals", Applied Physics Letter, Vol. 36, Number 11, pp 899-901, (1980).
61. N Itoh et.al., "17″ Video-Rate Full-Color FLCD", International Display Workshop'98, pp 205-208, (1998).
62. SID seminar lecture notes, Vol. 1, M-2/1-69, (1996).
63. C.H.Gooch and H.A.Tarry, "Optical Characteristics Of Twisted Nematic Liquid-Crystal Films", Electronics Letters, Vol. 10, Number 1, pp 2-4, (1974).
64. C.H.Gooch and H.A.Tarry, "The Optical Properties Of Twisted Nematic Liquid Crystal Structures With Twist Angles ≤ 90°", J.Phys.D: Applied Physics, Vol. 8, pp 1575-1584, (1975).
65. T.Sujiyama, Y.Toko, T Hashimoto, K Katoh, Y.Limura and S.Kobayashi, "Analytical Simulation Of Electrooptical Performance Of Amorphous Twisted Nematic Liquid

Crystal Displays", Japanese Journal of Applied Physics, Vol. 32, pp 5621-5632, (1993).

66. Pochi Yeh and Claire Gu, "Optics Of Liquid Crystal Displays", A Wiley Interscience Publication, John Wiley and Sons, Inc.
67. M.Schadt and F.Leenhouts, "Electro-Optical Performance Of A New, Black-White And Highly Multiplexable Liquid Crystal Displays", Applied Physics Letters, 50, pp 236-238, (1987).
68. Kazunori Katoh, Yukio Endo, Minoru Akatsuka, Masao Ohgawara and Kazutoshi Sawada, "Application Of Retardation Compensation; A New Highly Multiplexable Black-White Liquid Crystal Display With Two Supertwisted Nematic Layers", Japanese Journal of Applied Physics, Vol. 26, No. 11, pp L1784-L1786, (1987).
69. Scoichi Matsumoto, Hitoshi Hatoh, Akio Murayama, Tomiaki Yammoto, Susumu Kondo and Shinichi Kamagami, "A Single-Cell High Quality Black And White ST LCD", 8th International Display Research Conference (IDRC), pp 182-183, (1988).
70. S Togeshi, K Sekiguchi, H Tanabe, E Yamamoto, K Sorimachi, E Tajima, H Watanabe, H Shimizu, "LC–TV Display Controlled by A–Si Diode Rings", Proc.SID, Vol. 26-1, pp 9-15, (1985).
71. Donald E Castleberry, "Varistor-Controlled Liquid-Crystal Dispalys", IEEE Trans. Electron Devices, Vol. ED-26, No. 8, pp 1123-1128, (1979).
72. D R Baraff, John R Long, Blair K Maclaurin, Carla J Miner and Richard W Streater, "The Optimization of Metal-Insulator-Metal Nonlinear Devices for Use in Multiplexed Liquid Crystal Displays", IEEE Trans. Electron Devices, Vol. ED-28, No. 6, pp 736-739, (1981).
73. F C Luo, W A Hester and T P Brody, "Alphanumeric and Video Performance of a 6″×6″ 30 Lines-per-inch Thin-Film-Transistor – Liquid Crystal Display Panel", Digest of SID International Symposium, pp 94-85, (1978).
74. K.G. Beauchamp, "Applications of Walsh and related functions with an introduction to sequency theory", Academic press, London, (1984).

List of publications:

Techniques proposed in this thesis have been presented in the following publications.

1. K G Panikumar and T N Ruckmongathan, "An addressing technique for displaying restricted patterns in rms responding LCDs by selecting few rows at a time", Journal of the Society for Information Display, Vol. 8, No. 2, pp 155-162, (2000).

2. K G Panikumar and T N Ruckmongathan, "Displaying Gray Shades in Passive Matrix LCDs using Successive Approximation", Proceedings of the 7th Asian Symposium on Information Display (ASID'02), pp 229-232, (2002).

3. K G Panikumar and T N Ruckmongathan, "Driving matrix LCDs with reduced supply voltage and hardware complexity", Journal of the Society for Information Display, Vol. 10, No. 4, pp 363-373, (2002).

An addressing technique for displaying restricted patterns in rms-responding LCDs by selecting a few rows at a time

K. G. Pani Kumar
T. N. Ruckmongathan

Abstract — An addressing technique that will allow rms-responding matrix LCDs to display restricted patterns is proposed. This technique is based on the selection of a few rows at a time while scanning the display. In applications such as logic analyzers and oscilloscopes, mostly single-valued functions of time are displayed. This restriction in the image is useful in enhancing the selection ratio so that good contrast is achievable even with TN-LCDs. It is shown that a large reduction in the hardware complexity of the column drivers and the supply voltage is possible when the waveforms being displayed do not overlap each other and are equally spaced.

Keywords — *Passive-matrix LCDs, addressing technique, restricted pattern, multi-line addressing.*

1 Background

A matrix display is usually designed to display general patterns. Hence, it is possible to display 2^N different patterns in any column of a matrix display with N rows. However, most of these 2^N combinations do not occur in displays for oscilloscopes and logic analyzers. Shanks and Holland[1] have used the correlation properties of pseudo random binary sequence (PRBS) for displaying a single waveform on a matrix LCD. An infinite selection ratio is possible because only one waveform is displayed. An addressing technique for displaying multiple waveforms on a matrix LCD was proposed in 1986.[2] This technique is based on scanning the matrix by selecting one row at a time. The selection ratio of this technique is independent of matrix size and only depends on the number of waveforms (w) being displayed. In these displays the number of selected pixels in each column is equal to w. The number of background pixels (N-w) is usually much higher than w. The column voltage for the background pixels is chosen to be the same as that for the unselected rows. The column voltage for the selected pixels (*i.e.*, points on the waveform) is chosen to be in-phase with the row-select voltage. This is equivalent to assigning data 0 to the background pixel and +1 to the selected pixel. Here, the rms voltage of selected pixels is lower than that of the background pixels. Hence, this technique is referred to as the restricted pattern addressing technique – negative contrast (RPAT-NC).[3] The rms voltage across each selected pixel can also be made greater than the background pixel by choosing the column voltage for a selected pixels to be out of phase with the row-select voltage. This technique is referred to as the restricted pattern addressing technique – positive contrast (RPAT-PC). The selection ratios of RPATs are independent of matrix size and are higher than that of the conventional technique.[4] Hence, a good contrast ratio can be achieved even in LCDs with large matrix sizes. Instantaneous voltage across any pixel in a display addressed with RPATs is zero during most of the time intervals, and this may lead to flicker when N is very large. The supply-voltage requirement of RPATs also increases with matrix size. In order to overcome these problems a new flicker-free addressing technique was proposed in 1996.[5] This technique is based on selecting all the rows in the matrix display simultaneously, as in the case of active addressing.[6] Here the N rows in the matrix display are driven with waveforms corresponding to a set of orthogonal functions derived from PRBS. The column waveforms are generated by taking the orthogonal transform of the data to be displayed. Here, again, the data assigned to the background pixel is zero while +1 is assigned to the selected pixel. This technique is referred to as PRBS-NC. The lower rms voltage is supplied to the selected pixels compared to the background pixels. In a similar technique known as PRBS-PC, the selected pixels receive a higher rms voltage when the data assigned to the selected pixel is –1. A higher address duty factor in the PRBS techniques results in the suppression of flicker and frame response when N is large. The number of transitions in the row waveforms is almost the same when orthogonal functions derived from pseudo random binary sequence is used. This results in a good brightness uniformity of the pixels as compared to that of RPATs. The supply-voltage requirement in the PRBS techniques is independent of the matrix size, and it is lower than that of RPATs. The only disadvantage of PRBS techniques is that the number of voltage levels in the column waveform increases with w as in the case of displays in a logic analyzer.

In summary, both line-by-line addressing as well as simultaneous selection of all the rows has been considered

Received 7/31/00; accepted 9/21/00.

The authors are with the Raman Research Institute, Liquid Crystal Laboratory, Sir C. V. Raman Ave., Sadashivanagar, Bangalore, 560 080, India; telephone +91-80-3340124, fax +91-80-3340492, e-mail: pani@rri.ernet.in

in the past for displaying restricted pattern. We explored the possibility of selecting a few rows at a time. This approach is analogous to multi-line addressing (MLA) for displaying general patterns. We have found that it is possible to reduce the number of column voltage levels when the number of waveforms being displayed are large. Hence, it is possible to reduce the hardware complexity of the column drivers in special cases such as displays for a logic analyzer.

2 Technique

In this present work for displaying restricted patterns we have opted to scan the display by selecting a few rows at a time. This approach for driving matrix LCDs will be referred to as multi-line restricted pattern addressing (MLRPA). Here, the N rows to be multiplexed in a display are divided into (N/s) non-intersecting subgroups, with each subgroup consisting of s address lines. The data to be displayed in a selected subgroup in any one of the columns is an s-bit word represented d_{ks+i}. Here the value of i ranges from 1 to s and the variable k represents the selected subgroup and ranges from 0 to $[(N/s) - 1]$. By assigning the data for the background pixels to be 0, the selection ratio is independent of matrix size. Background pixels receive a higher rms voltage compared to the selected pixels when the data for the selected pixels is assigned to be +1. This results in negative contrast. The display exhibits a positive contrast when the data for the selected pixel is assigned to be −1. However, the selection ratio will be lower than that for the negative contrast mode. As in all the restricted-pattern addressing techniques, these two variants will be referred to as MLRPA – NC and MLRPA – PC, respectively.

A set of s orthogonal functions are used for selecting a subgroup of a matrix LCD. Simple orthogonal functions such as Walsh functions are preferred. Let $O(i,j)$ be the matrix representing the discrete version of the orthogonal functions. Here, the elements of the matrix $O(i,j)$ are just +1 or −1 and the following condition is satisfied:

$$\sum_{j=1}^{q} O(m,j)O(n,j) = \begin{cases} q & \forall m = n \\ 0 & \forall m \neq n \end{cases}, \qquad (1)$$

wherein q is the scaling factor which depends on the actual orthogonal matrix selected for scanning the display. In the case of Walsh functions and Hadamard matrices, q is the total number of columns in the orthogonal matrix. The columns of the orthogonal matrix $O(i,j)$ are called row-select patterns.

A subgroup is selected with voltages corresponding to one of the q row select patterns. The amplitude of these voltages is either $+V_r$ or $-V_r$ corresponding to +1 or −1 in the row-select pattern. The remaining $(N-s)$ rows of the unselected subgroups are grounded. The data in the selected subgroup is represented by a column vector, with elements taking values of 0 or +1. The column voltage is the

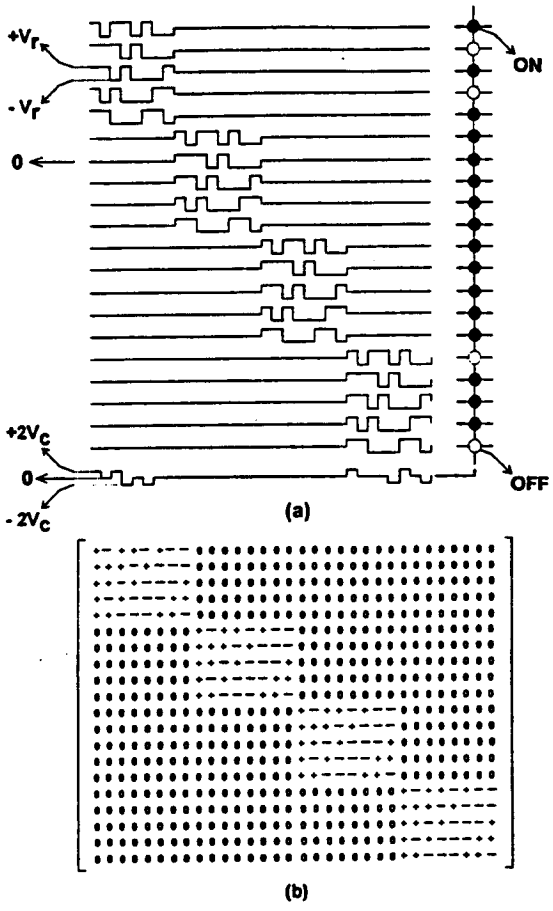

FIGURE 1 — Row-select pulses are adjacent to each other. (a) Row and column waveforms for a matrix LCD and (b) corresponding row select matrix. (Note: The symbols '+' represents a +1 and '−' represents a −1).

dot product of the row-select pattern and the data vector. This can be mathematically represented as

$$C_k(j) = \sum_{i=1}^{s} O(i,j)d_{ks+i} \qquad (2)$$

where $C_k(j)$ is the column voltage (normalized to V_c) corresponding to the j^{th} row-select pattern for the k^{th} subgroup. Similarly, column voltages for all the columns in the matrix are determined independently. Both the row and column voltages are applied simultaneously to the matrix display for a time duration τ. The process is repeated with another row-select pattern either in the same subgroup or a different subgroup. A cycle is completed when all the subgroups (N/s) are selected with all the row-select patterns once. The display is refreshed continuously by repeating this cycle. The scanning of the matrix can be done in a number of ways. The subgroup may be selected with all the row-select patterns once before selecting another subgroup. This is illustrated in Fig. 1, for $N = 20$ and $s = 5$. However, this method is not

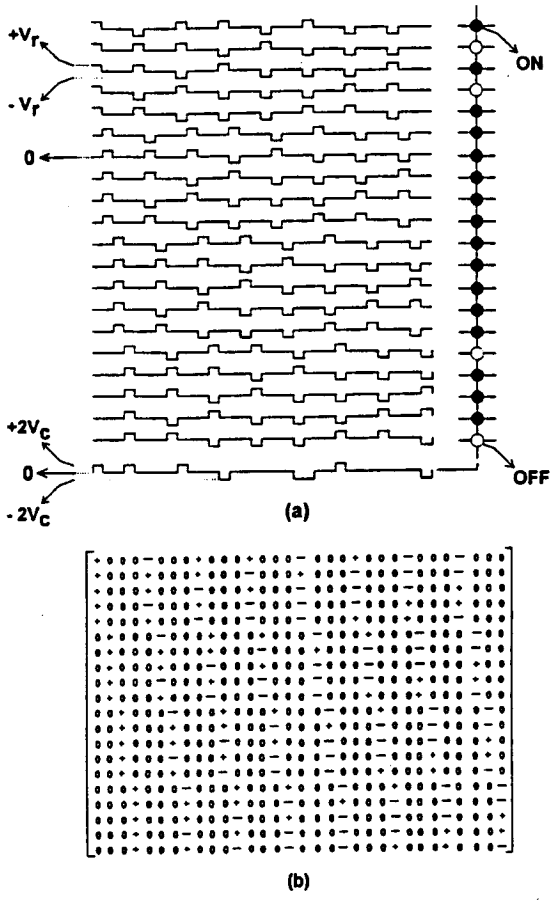

FIGURE 2 — The row-select pulses are distributed in a cycle. (a) Row and column waveforms for a matrix LCD and (b) corresponding row-select matrix. (Note: The symbols '+' represents a +1 and '–' represents a –1).

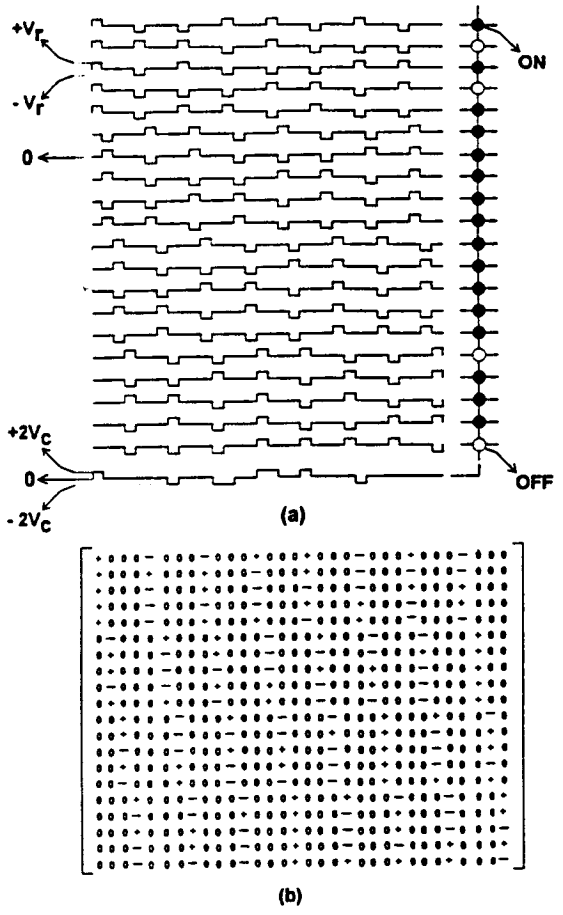

FIGURE 3 — The row-select pulses are distributed in a cycle by selecting a subgroup with different row select pattern. (a) Row and column waveforms for a matrix LCD and (b) corresponding row select matrix. (Note: The symbols '+' represents a +1 and '–' represents a –1).

suitable for fast-responding LCDs. Because the transmission of OFF pixels increases due to clustering of the usually large amplitude row-select pulses. This may lead to the *frame response phenomena*. In order to suppress the frame response, all the subgroups in the matrix LCD may be selected with one row-select pattern once before changing to another row-select pattern, as shown in Fig. 2. Good brightness uniformity of the pixel can be obtained by changing the row-select pattern whenever a new subgroup is selected. This is illustrated in Fig. 3.

3 Analysis

A subgroup is selected with voltages corresponding to one of the row-select patterns. The voltages are $+V_r$ or $-V_r$, corresponding to +1 or –1. The row voltage is zero during the $(N/s - 1)q$ time intervals when other rows are being selected. The column voltage $C_k(j)$ (normalized to V_c) which is the dot product of the row select pattern and the data vector in the k^{th} subgroup is given by

$$C_k(j) = \sum_{i=1}^{s} O(i,j)d_{ks+i},$$

where j ranges from 1 to q and k ranges from 0 to $N/s - 1$. The voltage across any pixel is the difference between row and column voltages. The rms voltage across the i^{th} pixel ($1 \le i \le s$) in the k^{th} subgroup [$0 \le k \le (N/s - 1)$] is given by

$$V_{ks+i}(rms) = \sqrt{\frac{\sum_{j=1}^{q}\left[V_r O(i,j) - C_k(j)\right]^2 + \sum_{\substack{n=0 \\ n\neq k}}^{(N/s-1)} \sum_{j=1}^{q}\left[C_n(j)\right]^2}{(N/s)q}} \qquad (3)$$

$$V_{ks+i}(rms) = \sqrt{\frac{\sum_{j=1}^{q}\left[(V_r O(i,j))^2 - 2V_r O(i,j)\sum_{i=1}^{s} O(i,j)d_{ks+i}\right] + \sum_{n=0}^{(N/s)-1}\sum_{j=1}^{q}\left[\sum_{i=1}^{s} O(i,j)d_{ns+i}\right]^2}{(N/s)q}}$$

$$V_{ks+i}(rms) = \sqrt{\frac{V_r^2\sum_{j=1}^{q}[O(i,j)]^2 - 2V_r d_{ks+i}\sum_{j=1}^{q}[O(i,j)]^2 + \sum_{n=0}^{(N/s)-1}\sum_{i=1}^{s}[d_{ns+i}]^2\sum_{j=1}^{q}[O(i,j)]^2}{(N/s)q}}$$

$$V_{ks+i}(rms) = \sqrt{\frac{V_r^2 q - 2V_r d_{ks+i} q + q\sum_{n=0}^{(N/s)-1}\sum_{i=1}^{s}[d_{ns+i}]^2}{(N/s)q}}. \quad (4)$$

This is the general expression for the multi-line addressing (MLA) technique. In order to display w waveforms in a matrix LCD, only w pixels in each column carry the information, and $(N\text{-}w)$ pixels in each column are the background pixels. Data for the w information carrying pixels are assigned to be +1, while the remaining $(N\text{-}w)$ background pixels are assigned to be 0. This results in a negative contrast (NC) mode, with selected pixels receiving a lower rms voltage compared to background pixels. If the $V_{ks+i}(rms)$ in Eq. (4) corresponds to the one for the selected pixel (*i.e.*, d_{ks+i} = +1), then the rms voltage across the selected pixel (*i.e.*, OFF) after simplification is

$$V_{off}(rms) = \sqrt{\frac{V_r^2 q - 2V_r q + wq}{(N/s)q}},$$

$$V_{off}(rms) = \sqrt{\frac{V_r^2 - 2V_r + w}{(N/s)}}. \quad (5)$$

Similarly, if $V_{ks+i}(rms)$ corresponds to a background pixel (*i.e.*, $d_{ks+i} = 0$), then from Eq. (4) the rms voltage across the background pixel (*i.e.*, ON) is

$$V_{on}(rms) = \sqrt{\frac{V_r^2 q + wq}{(N/s)q}},$$

$$V_{on}(rms) = \sqrt{\frac{V_r^2 + w}{(N/s)}}. \quad (6)$$

The selection ratio defined as $\left(V_{on}/V_{off}\right)$ is optimum when $V_r = \sqrt{w}$.

Thus, the optimum selection ratio for the MLRPA–NC mode is given by

$$SR = \sqrt{\frac{\sqrt{w}}{\sqrt{w}-1}}. \quad (7)$$

This selection ratio is same as that of RPAT–NC and PRBS–NC.

Similarly, by assigning data for the selected pixels to be –1 for the positive contrast mode, selection ratio for MLRPA–PC is given by

$$SR = \sqrt{\frac{\sqrt{w}+1}{\sqrt{w}}}. \quad (8)$$

This is same as that obtained for RPAT–PC and PRBS–PC techniques. Thus, the selection ratios for restricted pattern-addressing techniques are independent of the matrix size.

4 Supply voltage requirement of MLRPA–NC

The supply voltage (V_{sup}) for the driver is calculated by the maximum swing in the addressing waveforms as given below.

Case I:

If $(s \le \sqrt{w})$, then $2V_r > 2sV_c$, where $2V_r$ is the maximum swing in the row waveform and $2sV_c$ is the maximum swing in the column waveform. The supply voltage is given by

$$V_{sup} = 2V_r, \quad V_{sup} = 2\sqrt{w}\,V_c,$$

where

$$V_c = \sqrt{N/2ws}\,V_{sat},$$

i.e.,

$$V_{sup} = \sqrt{\frac{2N}{s}}\,V_{sat}. \quad (9)$$

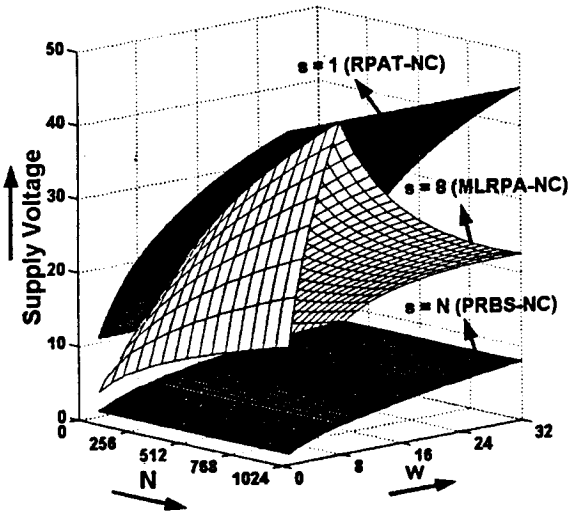

FIGURE 4 — Comparison of the supply voltage requirement (normalized to V_{sat}) for displaying restricted patterns using the MLRPA–NC technique when $s = 8$ with those of PRBS–NC and RPAT–NC.

Case II:

If $(\sqrt{w} < s < w)$, then the maximum swing in the addressing waveform is $2sV_c$, thus the supply voltage is

$$V_{sup} = 2sV_c,$$

$$V_{sup} = \sqrt{\frac{2Ns}{w}}V_{sat}. \quad (10)$$

Case III:

If $(s \geq w)$, then the maximum swing in the addressing waveform is $2wV_c$, the supply voltage is given by

$$V_{sup} = 2wV_c,$$

$$V_{sup} = \sqrt{\frac{2wN}{s}}V_{sat}. \quad (11)$$

Figure 4 shows a comparison graph of the supply voltage requirement for displaying restricted patterns for various values of N and w by selecting 8 rows at time.

5 Results

For case of the PRBS technique,[5] where in all the rows are selected simultaneously to display w waveforms, $(w + 1)$ column voltage levels are required. Hardware complexity of the column drivers also increases as the number of waveforms being displayed is increased. For the present MLRPA techniques, one can choose $s < w$ so that maximum number of column voltage levels can be limited to $s + 1$ instead of $w + 1$. Thus, the number of column voltage levels depends on the maximum number of selected pixels in the selected subgroups. However, usually not all the waveforms will overlap

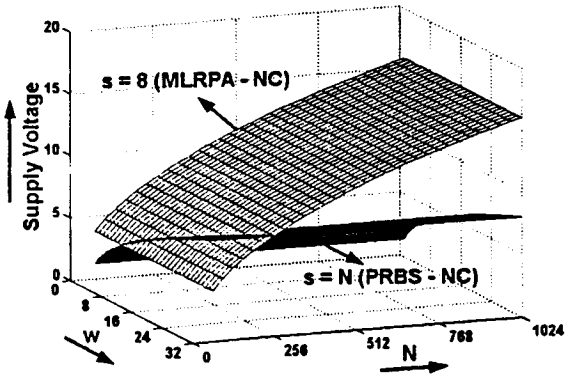

(a)

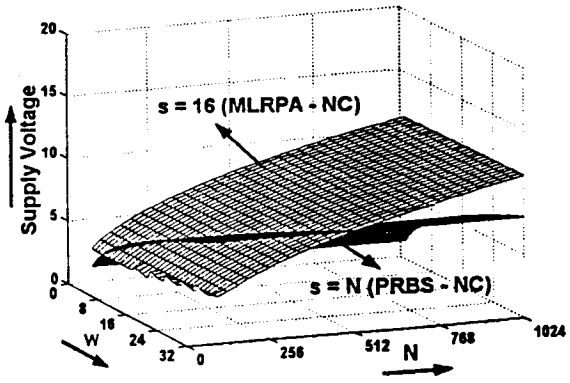

(b)

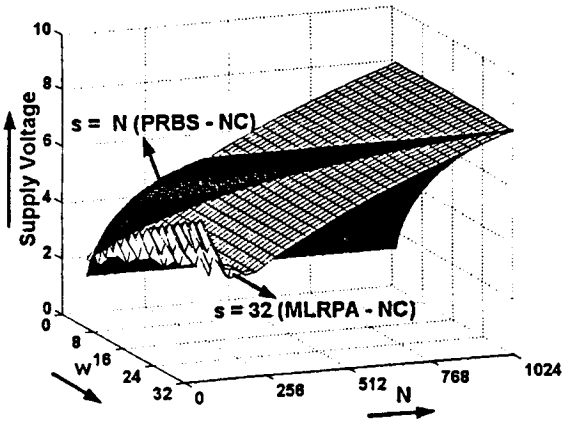

(c)

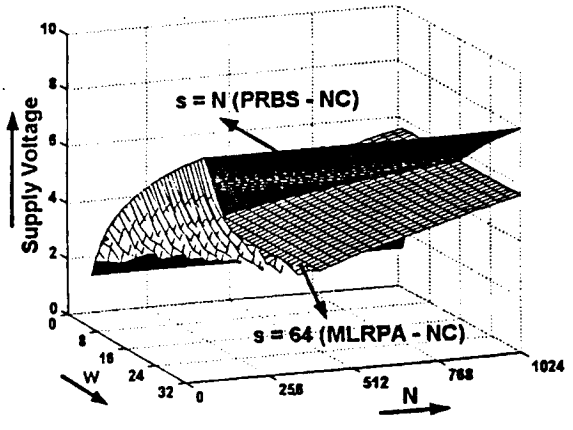

(d)

FIGURE 5 — (a) Comparison of the supply voltage requirement (normalized to V_{sat}) for displaying restricted pattern using the MLRPA–NC technique when $s = 8$ with that of PRBS–NC. (b) Comparison of the supply voltage requirement (normalized to V_{sat}) for displaying restricted patterns using the MLRPA–NC technique when $s = 16$ with that of PRBS–NC. (c) Comparison of the supply voltage requirement (normalized to V_{sat}) for displaying restricted patterns using the MLRPA–NC technique when $s = 32$ with that of PRBS–NC. (d) Comparison of the supply voltage requirement (normalized to V_{sat}) for displaying restricted patterns using the MLRPA–NC technique when $s = 64$ with that of PRBS–NC.

TABLE 1

N	w	MLRPA-NC Technique			PRBS-NC Technique		RPAT-NC
		s	No. of voltage levels required	Supply voltage (normalized to V_{sat})	No. of voltage levels required	Supply voltage (normalized to V_{sat})	No. of column voltage levels required (=4) Supply voltage (normalized to V_{sat})
64	4	8	3	4.000	5	2.8284	5.6569
		16	2	2.8284			
		32	3	2.000			
128	8	8	3	5.6569	9	4.0000	8.0000
		16	2	4.0000			
		32	3	2.8284			
		64	5	2.8284			
256	8	8	3	8.0000	9	4.0000	11.3137
		16	3	5.6569			
		32	2	4.0000			
		64	3	2.8284			
		128	5	2.8284			
	16	8	3	8.0000	17	5.6569	
		16	2	5.6569			
		32	3	4.0000			
		64	5	2.8284			
		128	9	4.0000			
512	16	8	3	11.3137	17	5.6569	16.0000
		16	3	8.0000			
		32	2	5.6569			
		64	3	4.0000			
		128	5	2.8284			
		256	9	4.0000			
	32	8	3	11.3137	33	8.0000	16.0000
		16	2	8.0000			
		32	3	5.6569			
		64	5	4.0000			
		128	9	4.0000			
		256	17	5.6569			

each other in a selected subgroup, and thus the number of column voltage levels may be less than $s + 1$.

In applications such as logic analyzers, the waveforms generally do not overlap with each other and are equally spaced. One can choose $N/s = w$, then only one selected pixel will be present in each subgroup. Hence, only two column voltage levels ($+V_c$ and $-V_c$) are required. If $(N/s) > w$, then in some subgroups none of the selected pixels may be present. Thus, only three column voltage levels ($+V_c$, 0 and $-V_c$) are needed. Hence, the number of column voltage levels can be reduced considerably for a given application.

Supply voltage for the drive electronics is given by the maximum swing in the addressing waveforms. Lower amplitude pulses reduce the supply voltage of the drive electronics. Figure 5 shows the supply voltage requirement (normalized to V_{sat}) of MLRPA–NC in comparison with PRBS-NC for various values of s.

Table 1 summarizes the number of column voltage levels as well as the supply voltage requirement of MLRPA–NC in comparison with that of the RPAT-NC and PRBS–NC techniques. A computer program has been developed to generate the data of row and column waveforms for a 256-row matrix LCD to display eight waveforms. The data from the program was loaded into the waveform

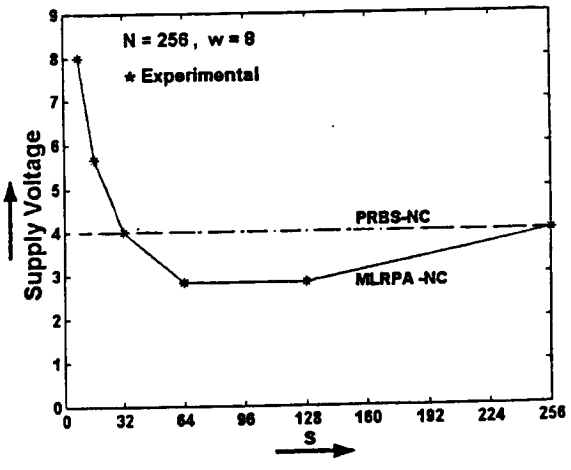

FIGURE 6 — Supply voltage (normalized to V_{sat}) of the MLRPA–NC technique for various values of s.

generator *"WFG 500,"* and typical row and column waveforms were applied to a single pixel. The supply-voltage requirement was measured using an electro-optic measurement setup. Figure 6 shows the supply-voltage requirement

TABLE 2

N	w	s	$[V_{sup}$(MLRPA–NC)/ V_{sup}(PRBS–NC)]×100	No of voltage levels required (MLRPA–NC)/ (PRBS–NC)
64	4	32	70.71	3/5
128	8	32	70.71	3/9
		64	70.71	5/9
256	8	64	70.71	3/9
		128	70.71	5/9
	16	32	70.71	3/17
		64	49.99	5/17
		128	70.71	9/17
512	16	64	70.71	3/17
		128	49.99	5/17
		256	70.71	9/17
	32	32	70.71	3/33
		64	50.00	5/33
		128	50.00	9/33
		256	70.71	17/33

(normalized to V_{sat}) for the case of the MLRPA–NC technique in displaying eight waveforms in a 256-row matrix LCD by selecting various values of s. The supply voltage obtained from the measurement agrees within ±1.5% of the theoretical values. The rms voltage across the ON and OFF pixels were measured using the HP 3467A, a logging multimeter capable of measuring true-rms voltage. Figure 7 shows the plot of V_{on} (rms) and V_{off} (rms) for various values of the supply voltage. Figure 8 shows the plot of the selection ratio measured experimentally. The selection ratio obtained from measurement agrees within ±0.5% of the theoretical value of 1.24375. Table 2 shows the value of s leading to a large reduction in the supply voltage as well as

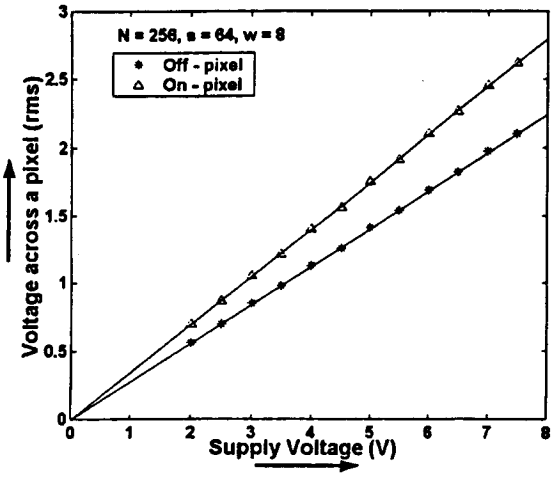

FIGURE 7 — *RMS* voltage across a pixel versus supply voltage.

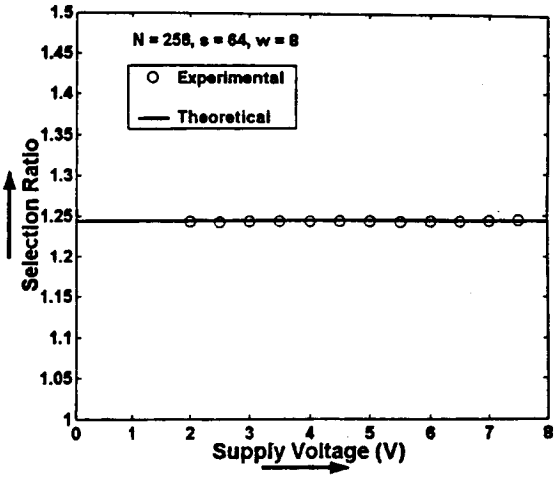

FIGURE 8 — Selection ratio versus supply voltage.

the number of column voltage levels for various values of N and w in comparison with the PRBS–NC technique. The addressing technique discussed above has been implemented using a 64 × 64 matrix TN-LCD. A photograph of a 64 × 64 display addressed by selecting eight rows at a time is shown in Fig. 9. Four waveforms are displayed with just three voltage levels in both row and column waveforms.

6 Conclusions

We have demonstrated the feasibility of a new addressing technique to display restricted patterns with TN-LCDs. The higher selection ratio of the restricted-pattern addressing technique allows for the use of relative fast TN-LCDs rather than STN-LCDs with slow response times. The

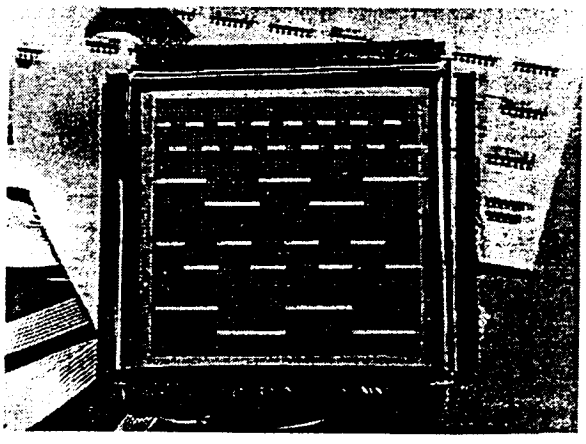

FIGURE 9 — Photograph of a 64 × 64 TN-LCD displaying four waveforms and addressed using MLRPA–NC by selecting eight rows at a time.

This figure is reproduced in color on page 184.

selection ratio which is independent of the matrix size is an added advantage of using restricted-pattern addressing to scan the passive-matrix LCD. The selection ratio of this multi-line approach is same as that for other restricted-pattern addressing techniques such as RPAT and PRBS. However, it is possible to reduce the hardware complexity of the column drivers as well as the supply-voltage requirement while using MLRPA by a careful choice of s for a given matrix size (N) and the number of waveforms (w).

Acknowledgment

The authors are thankful to S. Seshachala and H. Subramonyam for the fabrication of the display.

References

1 I A Shanks and P A Holland, "Addressing methods for non-multiplexed liquid crystal oscilloscope displays," *SID Intl Symp Digest Tech Papers*, 112-113 (1979).
2 T N Ruckmongathan, "An LCD for multitrace oscilloscope," *SID Intl Symp Digest Tech Papers*, 128-131 (1986).
3 T N Ruckmongathan, thesis submitted to department of electrical communication engineering, Indian Institute of Science, Bangalore, India, 1988.
4 P M Alt and P Pleshko, "Scanning limitations of liquid crystal displays," *IEEE Trans Electron Devices* **ED-21**, 146-155 (1974).
5 T N Ruckmongathan, "Flicker free restricted pattern addressing techniques with low supply voltage," *SID Intl Symp Digest Tech Papers*, 562-565 (1996).
6 T J Scheffer and B Clifton, "Active addressing method for high-contrast video-rate STN displays," *SID Intl Symp Digest Tech Papers*, 228-231 (1992).

Displaying Gray Shades In Passive Matrix LCDs Using Successive Approximation

K G Panikumar and T N Ruckmongathan

Raman Research Institute, Bangalore, India

ABSTRACT

The gray shades to be displayed in each pixel are represented as a g bit binary number and g time intervals are used to display any one of the 2^g gray shades. Amplitudes of the row and column waveforms of a passive matrix LCD are varied in different time intervals depending on the bit value of the gray shade data. Row and column voltages are reduced by a constant factor $1/\sqrt{2}$ as one scans the display using the most significant bit to the least significant bit. This results as a variation of RMS voltage across the pixels depending on the data and hence its gray shade. This has been achieved without any compromise on the selection ratio. In fact the standard drivers used for displaying bi-level (no gray shades) information are adequate if the voltage level generator is modified. For a given number of gray shades the flicker in the display is substantially less as compared to frame rate control method of displaying gray shades. Successive Approximation method has been used in conjunction with multi-line addressing (MLA) so as to keep the supply voltage low. The paper will describe the technique and present the experimental results.

Keywords: passive matrix, addressing technique, gray shade,

BACKGROUND

In the Super Twisted Nematic (STN) LCDs Frame Rate Control (FRC) [1] is widely used to display gray shades. In FRC f frames are used to display $(f + 1)$ gray shades. FRC uses standard row and column drivers to display gray shades. Flicker become visible as the number of gray shades increases. Pulse Width Modulation (PWM) [2] is also used to display gray shades. Here, each row select time is divided in to p time intervals to display $(p + 1)$ gray shades. Width of the pulses decrease as the number of gray shades increases. This leads to presence of high frequency components across the pixel resulting in brightness non-uniformity. Hence, the number of gray shades are limited in both these techniques. Amplitude Modulation (AM) [3] and Pulse Height Modulation (PHM) [4] may be used to display a large number of gray shades. However, the number of voltage levels in the column waveforms is high. Hence, analog type column drivers are necessary for displaying gray shades. The supply voltage of all these techniques while displaying gray shades is same as that for displaying bi-level information. Mano *et al.*, proposed the partial dispersion driving method [5] to display eight gray shades. Here, the amplitudes of the row waveforms were varied in the successive time intervals. The amplitude was reduced by a factor 2 in the successive time intervals from the most significant bit to the least significant bit. The selection ratio of this technique is lower than the maximum. The supply voltage increases when the amplitude of the row waveform is modulated in the successive time intervals. Hence they had demonstrated this technique in combination with multi-line addressing (MLA) to reduce the supply voltage and suppress the frame response. A Successive Approximation method is proposed in this paper to display gray shades without any compromise on the selection ratio.

TECHNIQUE

The N rows in a matrix display are divided into (N/s) non-intersecting subgroups. Each subgroup consists of s address lines. At a given instant of time a subgroup is selected with a row select pattern. The row select patterns are columns of an orthogonal matrix. This matrix is based on either hadamard matrices or walsh functions. The rest of the rows in the $(N/s - 1)$ subgroups are grounded. Here, a frame corresponds to selecting all the subgroups with all the row select pattern once. Only one of the g bits (of gray shade data) is considered during a frame. The column data is computed by taking the dot product between the row select pattern and the one bit of the data in the selected subgroup. Column data for all the columns are computed and shifted into the column drivers. The row and column voltages are multiplied by a factor C_f, wherein f corresponds to the bit position of the gray shade data. Both the row and column voltages are applied simultaneously to the matrix display for time duration τ. One frame is completed when all the subgroups are scanned with all the row select patterns once. As one can see, the scanning of the display is same as that for bi-level image except for the modulation of the row and column waveforms by C_f. In the next frame the scanning sequence is repeated by using the next bit as the data and the amplitudes of the row and column waveforms are multiplied by $C_{(f+1)}$. A cycle is complete when all the g bits of data and the corresponding g frames are used to scan the display once. Figure 1 shows the typical addressing waveforms of the Successive Approximation method in combination with the multi-line addressing technique. The waveforms in Figure 1 correspond to selecting a subgroup with all the row select patterns before moving on to the next subgroup. This has been shown to illustrate the waveforms of Successive Approximation clearly. However, both the subgroup and the row select

patterns were changed after selecting a subgroup with a row select pattern to ensure good brightness uniformity of pixels as shown in Figure 2.

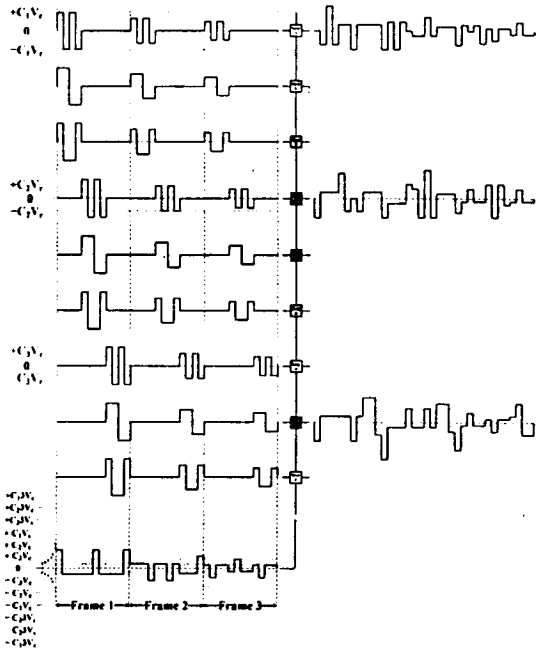

Figure 1. Typical addressing waveforms of Successive Approximation method in combination with MLA when $N = 9$, $s = 3$ and $g = 3$.

ANALYSIS

Gray shade of a pixel may be represented by

$$\sum_{f=1}^{g} d_{(g-f)}\, 2^{(g-f)} \qquad (1)$$

In the Successive Approximation technique the desired RMS voltage across the pixel is achieved by using g successive frames. The matrix display is scanned using one of the g bits (representing the gray shade value of the pixel) in each frame. The g frames corresponding to g bits (from MSB to LSB) form a cycle. The column signals are computed just as in the case of displaying bi-level information using one of the g bits. However, the amplitude of the row voltages are modified to $\pm C_f V_r$ instead of $\pm V_r$ and similarly the column voltages are multiplied by C_f corresponding to the f^{th} bit of the gray shade data. The matrix is scanned with these modified voltages. A cycle is complete when the matrix display is scanned by using the most significant bit to the least significant bit of the gray shade data with corresponding modulation (C_f) in the amplitudes of the row and column waveforms. The expression for square of the voltage across the i^{th} pixel in the k^{th} subgroup during a frame, when the matrix display is scanned with multi-line addressing[6] by selecting s rows and one bit data is given by the equation 2.

$$V_{ks+i}^2 = \left[\frac{q\,V_r^2 - 2\,q\,V_r V_c\,d(ks+i) + q\,N\,V_c^2}{q\,(N/s)}\right] \qquad (2)$$

Wherein, $d(ks+i)$ represents the data bit for the i^{th} row in the k^{th} subgroup for a given column. q is the number of columns in the orthogonal matrix.

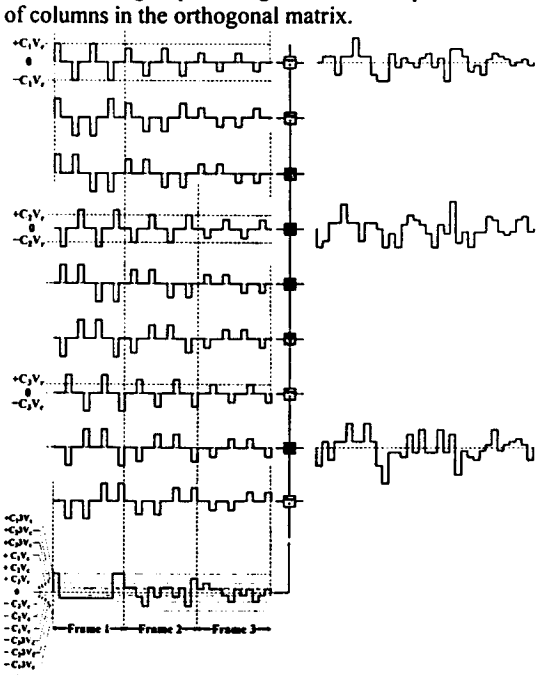

Figure 2. Typical addressing waveforms of Successive Approximation method in combination with MLA ($N = 9$, $s = 3$ and $g = 3$) when row select pulses are distributed in the frames.

Square of the voltage across the pixel during a frame with the modified row ($C_f V_r$) and column ($C_f V_c$) voltages is

$$V_{ks+i}^2 = \left[\frac{C_f^2\,q\,V_r^2 - 2\,C_f^2 q\,V_r\,V_c\,d_{(g-f)}(ks+i) + C_f^2\,q\,N\,V_c^2}{q\,(N/s)}\right]$$

$$V_{ks+i}^2 = \left[\frac{C_f^2\left(q\,V_r^2 - 2\,q\,V_r\,V_c\,d_{(g-f)}(ks+i) + q\,N\,V_c^2\right)}{q\,(N/s)}\right] \qquad (3)$$

The expression for the RMS voltage across a pixel in a cycle consisting of g frames is

$$V_{ks+i} = \sqrt{\frac{\sum_{f=1}^{g} C_f^2\left(q\,V_r^2 - 2q\,V_r V_c d_{(g-f)}(ks+i) + q\,N\,V_c^2\right)}{q\,g\,(N/s)}} \qquad (4)$$

The following condition needs to be satisfied

$\frac{C_f^2}{C_{f+1}^2} = 2$, wherein $C_f = \sqrt{2^{(g-f)}}$

The selection ratio is maximum when $V_r = \sqrt{N}\, V_c$ and the maximum selection ratio is $\sqrt{\frac{\sqrt{N}+1}{\sqrt{N}-1}}$. The RMS voltage across the ON and OFF pixels differ by a factor $\left(\sqrt{\frac{2^g-1}{g}}\right)$ as compared to the RMS voltages without any modulation. The OFF pixels in the display are biased near threshold voltage (V_{th}) in order to obtain a good contrast ratio. Hence, $V_{off} = V_{th}$

$$V_{off(RMS)} = \left(\sqrt{\frac{2^g-1}{g}}\right)\sqrt{\frac{\left[V_r^2 - 2\,V_r\,V_c + N\,V_c^2\right]}{\left(N/s\right)}} = V_{th}$$

$$V_c = \left(\sqrt{\frac{g}{2^g-1}}\right)\sqrt{\frac{N}{2\,s\left(N-\sqrt{N}\right)}}\;V_{th} \qquad (5)$$

Supply voltage requirement depends on maximum swing in the addressing waveforms across rows and columns. The maximum swing in the row waveform is greater than column waveforms when $N \geq s^2$ and is lesser than the column waveforms when $N \leq s^2$. The supply voltages for these two cases are given below.

Case I:

$$V_{sup} = 2\,C_1\,s\,V_c = 2\sqrt{2^{(g-1)}}\;s\,V_c \quad \text{for } N \leq s^2$$

$$V_{sup} = \sqrt{\frac{2\,s}{\left(1-1/\sqrt{N}\right)}\left(\frac{g\,2^{(g-1)}}{2^g-1}\right)}\;V_{th} \quad \text{for } N \leq s^2 \qquad (6)$$

Case II:

$$V_{sup} = 2\,C_1\,V_r = 2\sqrt{2^{(g-1)}}\sqrt{N}\;V_c \quad \text{for } N \geq s^2$$

$$V_{sup} = \sqrt{\frac{2\,N}{s\left(1-1/\sqrt{N}\right)}\left(\frac{g\,2^{(g-1)}}{2^g-1}\right)}\;V_{th} \quad \text{for } N \geq s^2 \qquad (7)$$

The supply voltage increases with g, i.e., gray shades being displayed. It increases by a factor $\sqrt{\frac{g\,2^{(g-1)}}{2^g-1}}$ as compared to the bi-level display. Figure 3 shows the increase in the supply voltage with respect to the number of bits g. This scaling factor is independent of the addressing technique used to scan the display. The supply voltage increases almost linearly with g. Supply voltage for displaying 256 gray shades is twice that of bi-level display. Supply voltage can be kept low by using MLA technique as compared to the conventional addressing technique. The number of voltage levels in the column waveform in a frame is (s+1), same as that of bi-level display.

The main advantage of Successive Approximation method is that both the row and column drivers used to drive the bi-level display can be used with a small modification in the voltage level generator (VLG) as shown in Figure 4.

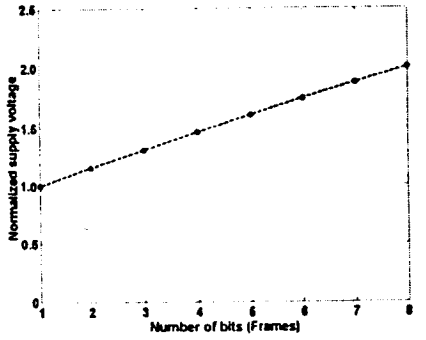

Figure 3. Supply voltage normalized to that of bi-level display versus number of bits.

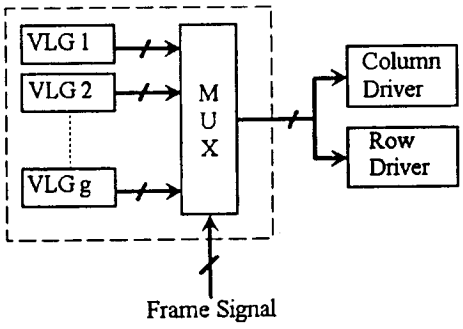

Figure 4. Modified voltage level generator for the Successive Approximation method to display gray shades.

RESULTS

The technique has been implemented using a 32x32 matrix TN-LCD by selecting three rows at time for displaying 16 gray shades. Figure 5 shows electro-optic response measured when Successive Approximation method is used for generating 16 gray shades. The RMS voltages across the pixels were measured using a logging multimeter (HP 3467A). Figure 6 shows the RMS voltage measured across the pixels versus supply voltage for these gray shades.

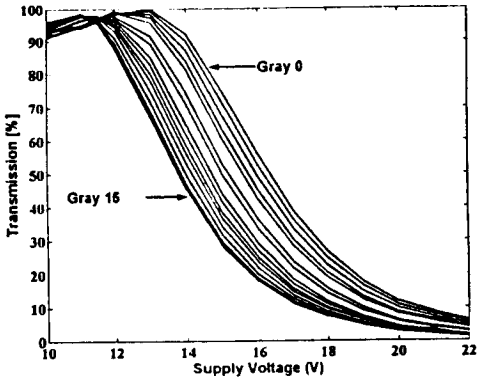

Figure 5. Light transmission versus supply voltage.

The RMS voltage across the ON and OFF pixels are plotted in figure 7 against the supply voltage. The selection ratio is also shown in the same figure. The selection ratio obtained from these measurement agrees within ±0.5% of the theoretical value of 1.1956.

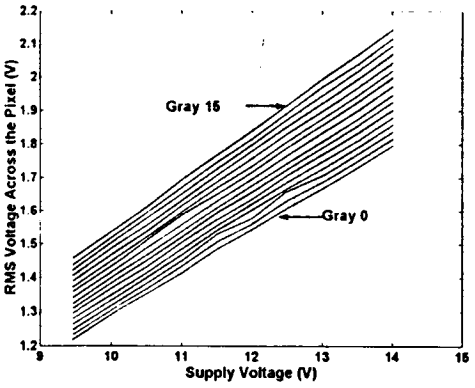

Figure 6. RMS voltage across a pixel versus supply voltage.

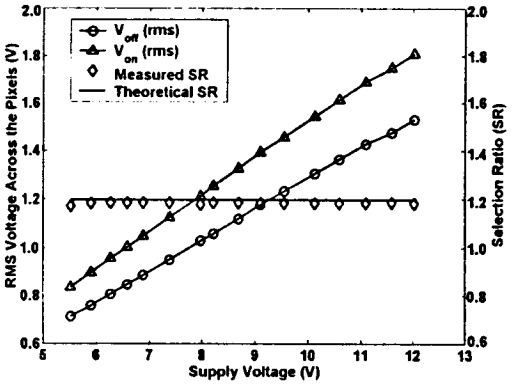

Figure 7. Selection ratio and RMS voltage across the ON and OFF pixels versus supply voltage.

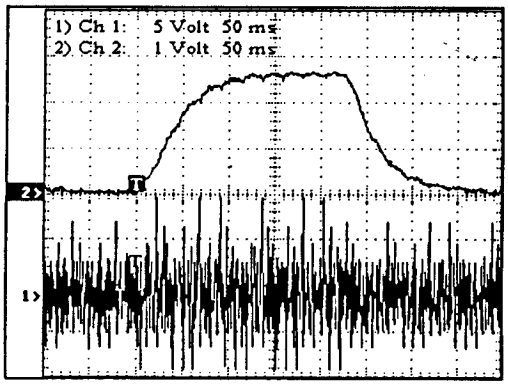

Figure 8. Electro-optic response of a pixel when switched between ON and OFF states.

Electro-optic response when a pixel is switched between On and OFF states is shown in Figure 8. The response time between OFF to ON and ON to OFF states are around 98 ms and 99 ms respectively. The response times when switching the pixels between the gray shades is given in Table 1. The first row and column of the Table 1 are the nine gray shades used for the measurement of the response times. A photograph of a 32×32 TN LCD for displaying 16 gray shades using Successive Approximation with four frames in a cycle is shown in figure 9.

Table 1. Response times (ms) between gray shades.

Gray Shade	0	2	4	6	8	9	11	13	15
0	-	109	122	118	113	109	112	98	98
2	99	-	113	112	95	112	112	101	88
4	117	89	-	98	95	104	89	101	93
6	107	98	110	-	96	92	96	89	87
8	96	86	98	79	-	82	76	84	82
9	97	96	99	102	84	-	83	72	69
11	102	105	94	93	77	79	-	71	62
13	91	91	99	85	74	65	85	-	49
15	99	92	111	92	92	80	52	56	-

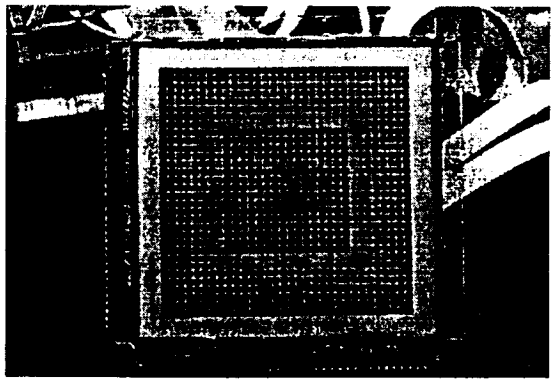

Figure 9. A 32x32 matrix LCD displaying gray shades using Successive Approximation method.

REFERENCES

1. Yoshio Suzuki, Mitsunobu Sekiya, Kunihiko Arai and Akio Ohkoshi, "A Liquid-Crystal Image Display", SID 83 Digest, pp. 32-33, (1983).
2. Hideaki Kawakami, Hisao Hanmura and Eiji Kaneko, "Brightness Uniformity in Liquid Crystal Displays", SID 80 Digest, pp. 28-29, (1980).
3. T N Ruckmongathan, "Addressing Technique for RMS Responding LCDs – A Review", Proc. of Japan Display'92, pp. 77-80, (1992).
4. A R Conner and T J Scheffer, "Pulse-Height Modulation (PHM) Gray Shading Methods for Passive Matrix LCDs", Proc. of Japan Display'92, pp. 69-72, (1992).
5. H Mano, S Nishitani K Kondo, J Taguchi and H Kawakami, "An Eight-Gray-Level Drive Method for Fast-Responding STN-LCDs", SID 93 Digest, pp. 93-96, (1993).
6. K G Panikumar and T N Ruckmongathan, "An addressing technique for displaying restricted pattern in rms-responding LCDs by selecting a few rows at a time", Journal of the SID, No. 8, Vol. 2, (2000).

Driving passive-matrix LCDs with low hardware complexity and reduced supply voltage

K. G. Panikumar
T. N. Ruckmongathan

Abstract — In passive-matrix liquid-crystal displays (LCDs), multiplexing is achieved by using the intrinsic non-linear characteristics of the liquid-crystal material. If the electro-optic characteristic is steeper than necessary for the matrix display, the selection ratio need not be maximized. Instead, the selection ratio can be reduced to match the electro-optic characteristics of the display. This leads to a reduction in the supply voltage of the drive electronics. We have considered the possibility of using addressing techniques with low hardware complexity along with displays having steep electro-optic characteristics. Supply voltages for these techniques are compared with that of multi-line addressing (MLA). The supply voltages of the Hybrid Addressing Technique (HAT), Improved Hybrid Addressing Technique-S3 (IHAT-S3), and Improved Hybrid Addressing Technique-S4 (IHAT-S4) are lower than that of MLA for the lower range of *N*. These hybrid addressing techniques with lower hardware complexity are a better choice for driving passive-matrix LCDs, especially in portable equipment.

Keywords *— Passive-matrix LCDs, addressing technique, multi-line addressing, hybrid addressing supply voltage.*

1 Background

The intrinsic non-linearity of the electro-optic effect is exploited to drive passive-matrix liquid-crystal displays (LCDs). During the last few decades, the addressing techniques for passive-matrix LCDs were optimized to achieve the maximum selection ratio. Selection ratio (SR) is defined as the ratio of the RMS voltage across an ON pixel (V_{on}) to that of an OFF pixel (V_{off}). Passive-matrix LCDs have been replaced by active-matrix LCDs in high-information-content applications requiring a large matrix size. Passive-matrix supertwisted nematic (STN) displays are now being used in mobile telephones, personal digital assistants (PDAs), and other medium- and low-information displays. In these applications, the matrix size is moderate and the electro-optic characteristics can be sharper than necessary. Supply voltage is another important parameter to be considered while using LCDs in portable devices. Several addressing techniques with low supply voltage have been proposed in the past (IHAT,[1] IHAT,[2] IHAT-S3, and IHAT-S4[3]). The supply voltage of an addressing technique is determined by the maximum swing in the addressing waveforms. Supply voltage is a minimum when the maximum swings in the row and column waveforms are equal. Supply voltage is a minimum for the case of the Improved Hybrid Addressing Technique (IHAT)[2] as well as Multi-Line Addressing (MLA)[4] when $s = N^{1/2}$. Here, N is the total number of lines being scanned in a matrix LCD and s is the number of rows in the subgroups. The supply-voltage requirement can be further

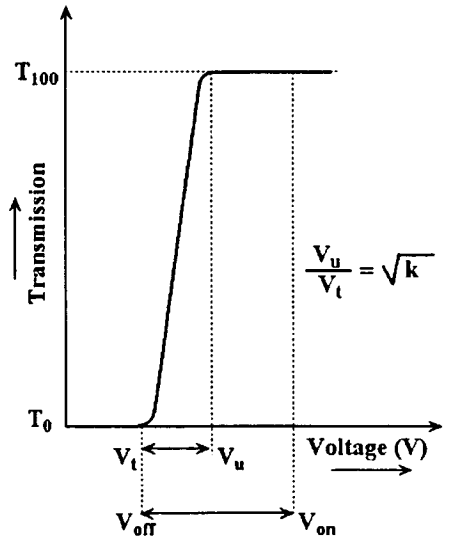

FIGURE 1 — Electro-optic characteristics curve ($V_{on} > V_u$).

TABLE 1 — Column voltages for the various hybrid addressing techniques.

Technique	Mismatches (i)	Column Voltage (V_c)
HAT (odd s)	$i < (s/2)$	$+V_c$
	$i > (s/2)$	$-V_c$
IHAT-S3 (even s)	$0 \le i \le m$	$+V_m$
	$m < i < (s-m)$	0
	$(s-m) \le i \le s$	$-V_m$
IHAT-S4 (odd s)	$0 \le i \le m_1$	$+V_{m1}$
	$m_1 < i < s/2$	$+V_{m2}$
	$s/2 \le i \le (s-m_1)$	$-V_{m2}$
	$(s-m_1) \le i \le s$	$-V_{m1}$

The authors are with the Raman Research Institute, Liquid Crystal Laboratory, Sir C. V. Raman Ave., Sadashivanagar, Bangalore 560 080 India; telephone +91-80-3610124, fax +91-80-3610492, e-mail: ruck@rri.res.in.

TABLE 2 — The coefficents α, β, γ, and δ for the various hybrid addressing techniques.

Technique	α	β	γ	δ
HAT	2^s	$2(4P-2^s)$	$2^s\left(\frac{N}{s}\right)$	$2^s\left(\frac{N}{s}\right)$
IHAT	2^s	$2\left(\frac{2^s}{s}\right)$	$2^s\left(\frac{N}{s^2}\right)$	$2^s\left(\frac{N}{s}\right)$
IHAT-S3	2^{s-1}	$2\left[\sum_{i=0}^{m}(A_i-B_i)\right]$	$\frac{N}{s}\left[\sum_{i=0}^{m}(A_i+B_i)\right]$	$2^{s-1}\left(\frac{N}{s}\right)$
IHAT-S4	2^{s-1}	$2\left[\left(\sum_{i=0}^{ml}(A_i-B_i)\right)+\frac{DG}{EF}\left(\sum_{i=ml+1}^{(s-1)/2}(A_i-B_i)\right)\right]$	$\frac{N}{s}\left[\left(\sum_{i=0}^{ml}(A_i+B_i)\right)+\left(\frac{DG}{EF}\right)^2\left(\sum_{i=ml+1}^{(s-1)/2}(A_i+B_i)\right)\right]$	$2^{s-1}\left(\frac{N}{s}\right)$
MLA	q	$2\left(\frac{q}{s}\right)$	$q\left(\frac{N}{s^2}\right)$	$q\left(\frac{N}{s}\right)$

where

$$A_i=\frac{(s-1)!}{i!(s-i-1)!} \qquad B_i=\frac{i(s-1)!}{i!(s-i)!} \qquad P=\sum_{i=0}^{(s-1)/2}A_i$$

$$D=\sum_{i=0}^{ml}(A_i+B_i) \qquad E=\sum_{i=ml+1}^{(s-1)/2}(A_i+B_i) \qquad F=\sum_{i=0}^{ml}(A_i-B_i)$$

$$G=\sum_{i=ml+1}^{(s-1)/2}(A_i-B_i)$$

and q is the total number of time intervals in the orthogonal matrix used in the case of MLA.

reduced by following the scheme proposed by Kuijk (1999).[5] Here, the electro-optic characteristic is steeper than necessary for the matrix size. The difference between the RMS voltage across the ON and OFF pixels is more than necessary for multiplexing N rows of the matrix LCD as shown in Fig. 1. The voltage across the ON pixel can be lowered to V_u without affecting the contrast of the display. Hence, the selection ratio is reduced to V_u/V_t and is referred to as the reduced selection ratio. This will help to lower the supply voltage of the drive electronics without losing contrast. We have considered HAT, IHAT-S3, and IHAT-S4 with a low hardware complexity of drivers. The selection ratios of these techniques are lower than the maximum value due to the restrictions imposed on the number of voltage levels in the column waveforms. A lower selection ratio is not a problem since the electro-optic characteristic of the liquid crystal is steep enough for the small or moderate number of rows being multiplexed. The number of voltage levels in the column waveforms is restricted to two, three, and four in the cases of HAT, IHAT-S3, and IHAT-S4, respectively, as compared to $(s + 1)$ in the case of IHAT[2] or MLA[4]. The supply-voltage requirements of these techniques are compared with that of the multi-line addressing technique[5] when the selection ratio is reduced to match the electro-optic characteristic.

2 Hybrid addressing techniques

In the hybrid addressing techniques, the N rows in the matrix are divided into (N/s) non-intersecting subgroups with each subgroups consisting of s address lines. At a given instant of time, one subgroup is selected with voltages corresponding to an s-bit row select pattern. Here, a row select pattern corresponds to one of the 2^s binary patterns. The amplitudes of these voltages are either $+V_r$ for logic 0 and $-V_r$ for logic 1. The remaining $(N - s)$ unselected rows are grounded. The data to be displayed in the selected subgroup in any column is also an s-bit word with logic 0 representing an OFF pixel and logic 1 for an ON pixel. The column voltage is decided by the number of mismatches[1,3]

between the row select pattern and the data in the selected subgroup. The number of mismatches i is given by

$$i = \sum_{j=1}^{s} a_j \oplus d_{ks+j}, \tag{1}$$

where $(a_1,a_2,a_3,\ldots a_s)$ is an s–bit row select pattern and d_{ks+j} is the data in the k^{th} subgroup $[k = 0,1,2, \ldots (N/S - 1)]$. Table 1 gives the column voltages for the various hybrid addressing techniques. The mismatches for all the columns in the matrix are computed and transferred to the column driver. Then both the row and column voltages are applied simultaneously to the matrix display for a time duration τ. The process is repeated with another row select pattern by selecting the same subgroup or a different subgroup. A cycle is completed when all the subgroups (N/s) are selected with all the 2^s row-select patterns once. The display is refreshed continuously by repeating this cycle.

Expressions for the RMS voltage across the ON and OFF pixels are of the form shown in Eqs. (2) and (3):

$$V_{on} = \sqrt{\frac{\alpha V_r^2 + \beta V_r V_c + \gamma V_c^2}{\delta}}, \tag{2}$$

$$V_{off} = \sqrt{\frac{\alpha V_r^2 - \beta V_r V_c + \gamma V_c^2}{\delta}}. \tag{3}$$

The coefficients α, β, γ, and δ for the various hybrid addressing techniques are given in Table 2.

With a steep electro-optic characteristic, the selection ratio can be reduced to V_u/V_t. Hence, the reduced selection ratio is

$$SR_{reduced} = \frac{V_u}{V_t} = \sqrt{k}. \tag{4}$$

The condition for the reduced selection ratio is determined as follows:

$$SR_{reduced} = \frac{V_{on}}{V_{off}} = \sqrt{\frac{\alpha V_r^2 + \beta V_r V_c + \gamma V_c^2}{\alpha V_r^2 - \beta V_r V_c + \gamma V_c^2}} = \sqrt{k}.$$

This expression can be simplified to

$$SR_{reduced} = \sqrt{\frac{\alpha x^2 + \beta x + \gamma}{\alpha x^2 - \beta x + \gamma}} = \sqrt{k},$$

wherein $x = V_r/V_c$. Solving for x, we get

$$x = \frac{\beta}{2\alpha}\left(\frac{k+1}{k-1}\right) \pm \sqrt{\left[\frac{\beta}{2\alpha}\left(\frac{k+1}{k-1}\right)\right]^2 - \frac{\gamma}{\alpha}}. \tag{5}$$

The RMS voltage across the OFF pixels is controlled to be near V_{th} in order to get a good contrast ratio in the display. Hence,

TABLE 3 — The coefficients α, β, γ, and δ of the hybrid addressing techniques for two differnet values of s.

Technique	s	α	β	γ	δ	Column voltage levels with grouping of mismatches (i) for highest SR possible
HAT	3	8	8	$\frac{8N}{3}$	$\frac{8N}{3}$	(0,1) $+V_c$ | (2,3) $-V_c$
	5	32	24	$\frac{32N}{5}$	$\frac{32N}{5}$	(0,1,2) $+V_c$ | (3,4,5) $-V_c$
IHAT-S3	4	8	6	$\frac{5N}{4}$	$\frac{8N}{4}$	(0,1) $+V_c$ | (2) 0 | (3,4) $-V_c$
	6	32	20	$\frac{11N}{3}$	$\frac{16N}{3}$	(0,1,2) $+V_c$ | (3) 0 | (4,5,6) $-V_c$
IHAT-S4	5	16	$\frac{46}{5}$	$\frac{69N}{50}$	$\frac{16N}{5}$	(0,1) $+V_c$ | (2) $+\left(\frac{3}{10}\right)V_c$ | (3) $-\left(\frac{3}{10}\right)V_c$ | (4,5) $-V_c$
	7	64	$\frac{688}{21}$	$\frac{9976N}{2205}$	$\frac{64N}{7}$	(0,1,2) $+V_c$ | (3) $+\left(\frac{145}{525}\right)V_c$ | (4) $-\left(\frac{145}{525}\right)V_c$ | (5,6,7) $-V_c$

TABLE 4 — The minimum supply voltage (normalized to V_{th}) with reduced selection ratios for various values of s.

Technique	Reduced selection ratio	s	N_{min}(HA) ($x \equiv 1$)	V_{sup} (normalized to V_{th})	MLA	
					N_{min}(MLA) ($x \equiv 1$)	V_{sup} (normalized to V_{th})
HAT	1.1055	3	27	2.0000	51	3.3665
		5	30	1.9760	75	4.0825
	1.0668	3	42	2.0025	84	3.4059
		5	50	1.9828	130	4.2373
IHAT-S3	1.1055	4	40	2.4911	64	3.7712
		6	42	2.3525	84	4.3205
	1.0668	4	68	2.5020	108	3.8620
		6	72	2.3692	150	4.5518
IHAT-S4	1.1055	5	55	2.9183	75	4.0825
		7	56	2.7047	92	4.5766
	1.0668	5	90	2.9707	130	4.2373
		7	98	2.7481	168	4.8174

$$V_{off} = \sqrt{\frac{\alpha x^2 - \beta x + \gamma}{\delta}} V_c = V_{th},$$

$$V_c = \sqrt{\frac{\delta}{\alpha x^2 - \beta x + \gamma}} V_{th}. \quad (6)$$

The supply voltage is determined by the maximum swing in the addressing waveforms. The expressions for the supply voltage are

$$V_{sup} = 2V_c \quad \text{for} \quad V_r \le V_c,$$

$$V_{sup} = 2\sqrt{\frac{\delta}{\alpha x^2 - \beta x + \gamma}} V_{th} \quad \text{for} \quad V_r \le V_c, \quad (7)$$

$$V_{sup} = 2V_r = 2xV_c \quad \text{for} \quad V_r \ge V_c,$$

$$V_{sup} = 2x\sqrt{\frac{\delta}{\alpha x^2 - \beta x + \gamma}} V_{th} \quad \text{for} \quad V_r \ge V_c. \quad (8)$$

The coefficients α, β, γ, and δ of the hybrid addressing techniques for two different values of s are shown in Table 3. The column voltages of IHAT-S3 and IHAT-S4 have several possible values depending on the grouping of mismatches.[3] We have considered the grouping leading to the highest selection ratio. Both the grouping of mismatches and the corresponding voltage levels[3] are also shown in Table 3. Supply voltage is a minimum when the maximum swings in the addressing waveforms (row and column) are equal (when $x = V_r/V_c$ is 1); that is, when

$$\gamma = \beta\left(\frac{k+1}{k-1}\right) - \alpha. \quad (9)$$

Table 4 shows the minimum supply voltage (normalized to V_{th}) with reduced selection ratios for various values of s.

3 Results and discussions

Supply voltages of HAT, IHAT, IHAT-S3, and IHAT-S4 with a reduced selection ratio are compared with the results of Kuijk[5] for MLA. The IHAT has the same reduction in supply voltage as that of the MLA technique.[5] This is expected since the row-select patterns of MLA are a subset of the row select patterns of IHAT.[6] The number of time intervals to complete a cycle is the only parameter that differs between IHAT and MLA while all other parameters like supply voltage, selection ratio, *etc.*, are the same for IHAT and MLA. Two different liquid-crystal mixtures were considered to compute the supply voltage for the hybrid addressing techniques. Liquid-crystal mixture 1 (LC1), suitable for multiplexing 100 lines, *i.e.* $(V_u/V_t) = 1.1055$, and liquid-crystal mixture 2 (LC2), capable of multiplexing 240 lines, *i.e.*, $(V_u/V_t) = 1.0668$, were considered for the analysis. Supply voltages for HAT, IHAT-S3, and IHAT-S4 were calculated for different matrix sizes (N). The minimum supply voltage

TABLE 5 — The number of address lines for which supply voltages of HAT, IHAT-S3, and IHAT-S4 are almost equal to that of MLA (N_{eqs}).

Technique	Reduced selection ratio	s	N_{eqs}	V_{sup} (normalized to V_{th})
HAT	1.1055	3	44	3.4115
		5	61	4.1527
	1.0668	3	72	3.4008
		5	108	4.2979
IHAT-S3	1.1055	4	60	3.7534
		6	77	4.4337
	1.0668	4	102	3.8616
		6	138	4.5963
IHAT-S4	1.1055	5	73	4.0752
		7	87	4.5592
	1.0668	5	127	4.2384
		7	161	4.8306

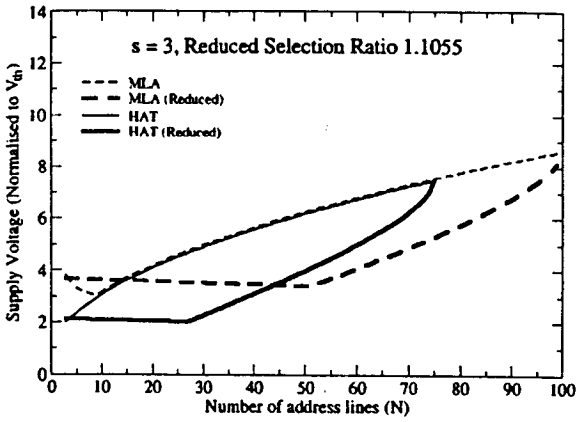

FIGURE 2 — Supply voltage (normalized to V_{th}) *vs.* N for HAT and MLA when s = 3 and SR = 1.1055.

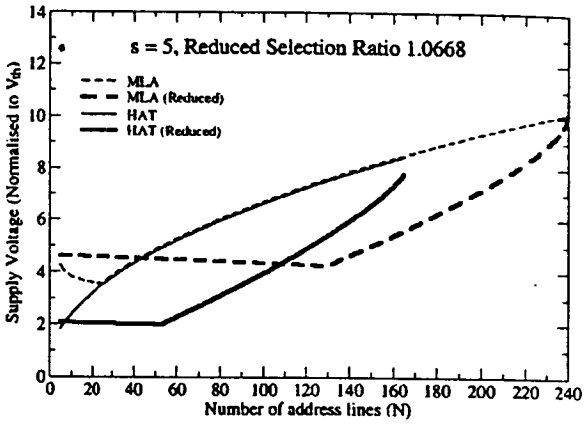

FIGURE 5 — Supply voltage (normalized to V_{th}) *vs.* N for HAT and MLA when s = 5 and SR = 1.0668.

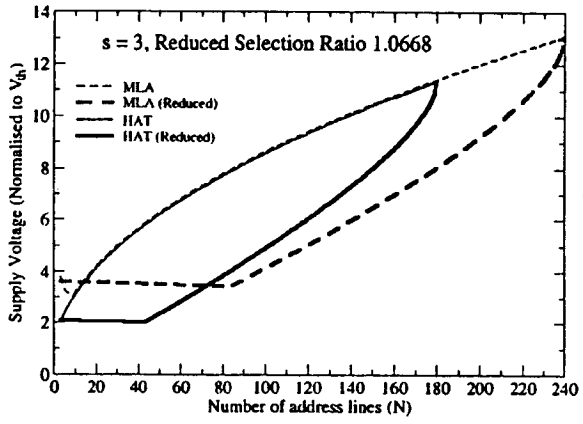

FIGURE 3 — Supply voltage (normalized to V_{th}) *vs.* N for HAT and MLA when s = 3 and SR = 1.0668.

is achieved when the maximum swings in the row and column waveforms are equal. Table 4 gives the number of lines being multiplexed when the supply voltage is a minimum (N_{min}) for hybrid addressing N_{min}(HA) and multi-line addressing N_{min}(MLA). Supply voltages of HAT, IHAT-S3, and IHAT-S4 are less than that for MLA over certain ranges of N. Figures 2–13 show the supply voltage (normalized to V_{th}) *vs.* the number of address lines (N) for two s values in the case of HAT, IHAT-S3, and IHAT-S4 as compared to MLA.[5] The supply voltage of MLA when the selection ratio is a maximum has also been plotted for comparison. The number of address lines for which supply voltages of HAT, IHAT-S3, and IHAT-S4 are almost equal to that of MLA (N_{eqs}) are shown in Table 5. The supply voltage of hybrid addressing is lower than that of MLA when N (the number of lines being multiplexed) is less than N_{eqs}. A good reduction in supply voltage is achieved when N is less than N_{min}(HA). The percentage reduction in supply voltage com-

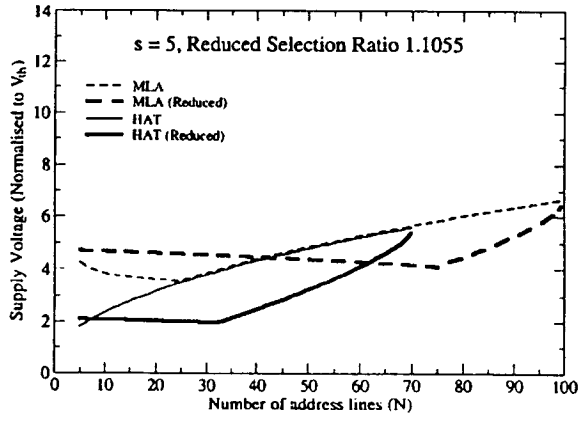

FIGURE 4 — Supply voltage (normalized to V_{th}) *vs.* N for HAT and MLA when s = 5 and SR = 1.1055.

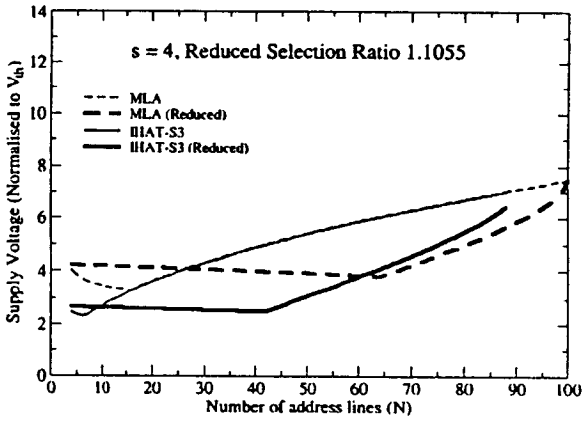

FIGURE 6 — Supply voltage (normalized to V_{th}) *vs.* N for IHAT-S3 and MLA when s = 4 and SR = 1.1055.

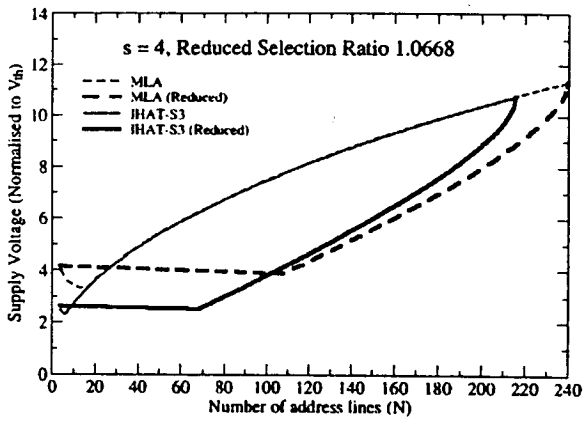

FIGURE 7 — Supply voltage (normalized to V_{th}) *vs.* N for IHAT-S3 and MLA when $s = 4$ and SR = 1.0668.

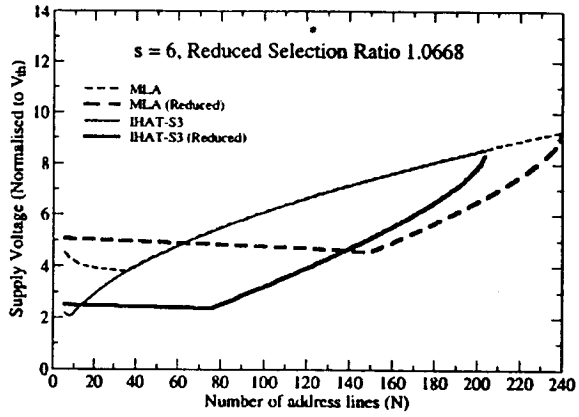

FIGURE 9 — Supply voltage (normalized to V_{th}) *vs.* N for IHAT-S3 and MLA when $s = 6$ and SR = 1.0668.

pared with MLA[5] is almost constant when N is less than or equal to N_{min}(HA):

$$\text{percentage reduction} = \frac{V_{sup}(\text{MLA}) - V_{sup}(\text{HA})}{V_{sup}(\text{MLA})} \times 100.$$

This reduction in supply voltage is plotted in Fig. 14 for the various hybrid addressing techniques. Table 6 gives the maximum reduction (percentage) in supply voltage compared to the MLA[5] technique when N is equal to N_{min}(HA).

The supply voltage for line-by-line addressing may also be reduced by lowering the selection ratio to match the electro-optic characteristics. The supply voltages of the Alt and Pleshko Technique[7] (APT) and the Improved Alt and Pleshko Technique[8] (IAPT) are the same for lower values of N (in the region where the reduced row select pulse $V_{r(\text{reduced})} \leq V_{c(\text{reduced})}$). The supply voltages for APT and IAPT are almost equal to that of HAT as shown in Figs. 15 and 16 in the region $V_{r(\text{reduced})} \leq V_{c(\text{reduced})}$. The supply voltage is

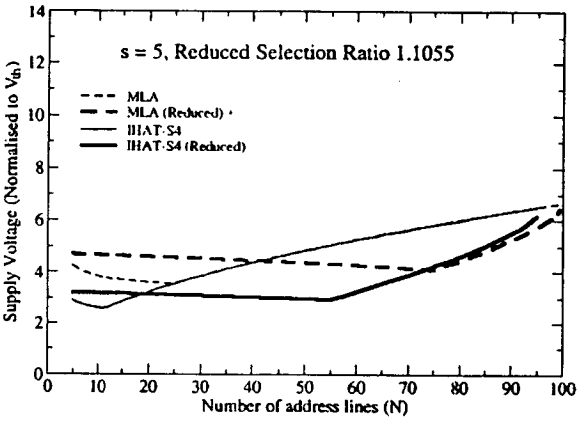

FIGURE 10 — Supply voltage (normalized to V_{th}) *vs.* N for IHAT-S4 and MLA when $s = 5$ and SR = 1.1055.

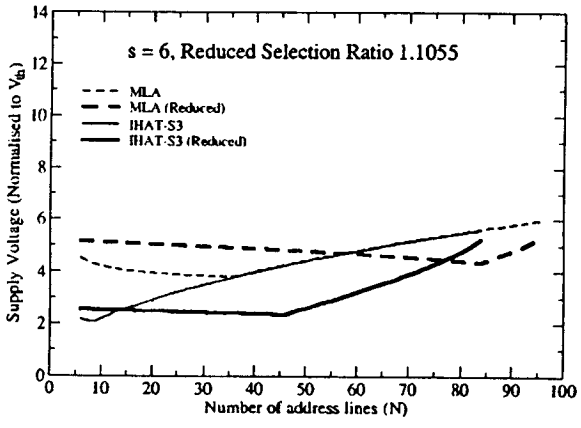

FIGURE 8 — Supply voltage (normalized to V_{th}) *vs.* N for IHAT-S3 and MLA when $s = 6$ and SR = 1.1055.

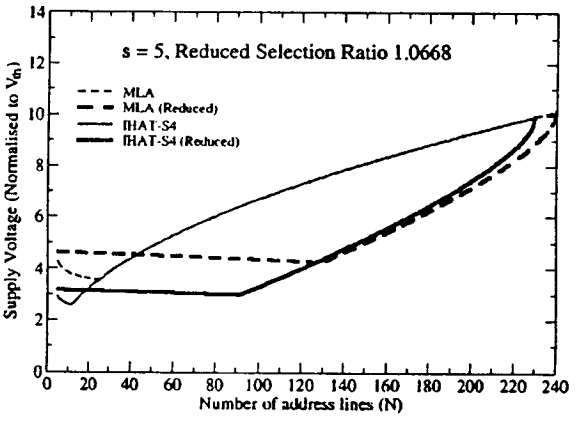

FIGURE 11 — Supply voltage (normalized to V_{th}) *vs.* N for IHAT-S4 and MLA when $s = 5$ and SR = 1.0668.

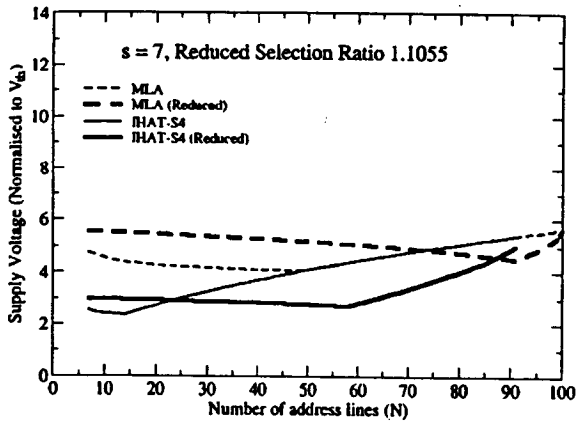

FIGURE 12 — Supply voltage (normalized to V_{th}) *vs.* N for IHAT-S4 and MLA when $s = 7$ and SR = 1.1055.

a minimum when the amplitudes of row and column waveforms are equal (when $N = 19$ and $N = 30$ for the liquid-crystal mixtures LC1 and LC2, respectively). A comparison of the lowered supply voltages of hybrid addressing techniques with that of APT, IAPT, and MLA with reduced selection ratios is shown in Figs. 15 and 16. The hybrid addressing techniques show a good reduction in supply voltage. The addressing techniques which have the lowest supply voltage and the range of N over which the supply voltage is low are given in Tables 7 and 8 for LC1 and LC2, respectively. The hybrid addressing technique (HAT) has low hardware complexity (two voltage levels in the column waveforms and three voltage levels in the row waveforms) and has the lowest supply voltage for the lower values of N. IHAT-S3 and S4 have the lowest supply voltage for the mid-range of N, while IHAT as well as MLA have the lowest supply voltage for the higher values of N. Active addressing[9] wherein all the rows are selected simultaneously requires the same supply voltage as APT. The hardware complexity of column drivers and

TABLE 6 — The maximum reduction (percentage) in supply voltage compared to the MLA technique when N is equal to N_{min}(HA).

Technique	s	Reduced selection ratio	N_{min}(HA)	$\left(\frac{V_{sup}(MLA) - V_{sup}(HA)}{V_{sup}(MLA)}\right)$ 100 %
HAT	3	1.1055	27	43.1181
		1.0668	42	42.7758
	5	1.1055	30	56.2569
		1.0668	50	55.8848
IHAT-S3	4	1.1055	40	37.2776
		1.0668	68	37.0377
	6	1.1055	42	51.4586
		1.0668	72	51.1898
IHAT-S4	5	1.1055	55	32.2687
		1.0668	90	32.0971
	7	1.1055	56	46.8262
		1.0668	98	46.5939

the controller is high for active addressing, so this technique is not attractive for practical implementation even though the reduced supply voltage is also same as that of APT.

The row and column waveforms of HAT, IHAT-S3, and IHAT-S4 were generated using the waveform-generator *WFG 500* for various values of s and N in order to verify the results experimentally. The RMS voltage across the ON and OFF pixels were measured using the HP 3467A, a logging multimeter capable of measuring true RMS voltage. Tables 9–11 show the measured RMS voltages and the percentage of error as compared to the theoretical value for different values of N and s for the cases of HAT, IHAT-S3, and IHAT-S4. The RMS voltages and the selection ratios obtained from these measurements agree within ±0.8% of the theoretical values.

The hybrid addressing techniques have a lower supply voltage. The hardware complexity of the column drivers of these techniques is lower than that for IHAT and MLA. It is important to note that the higher number of time intervals to complete a cycle for the hybrid addressing techniques compared to MLA is not a disadvantage. In fact, the Hadamard as well as the Walsh matrices are subsets of the

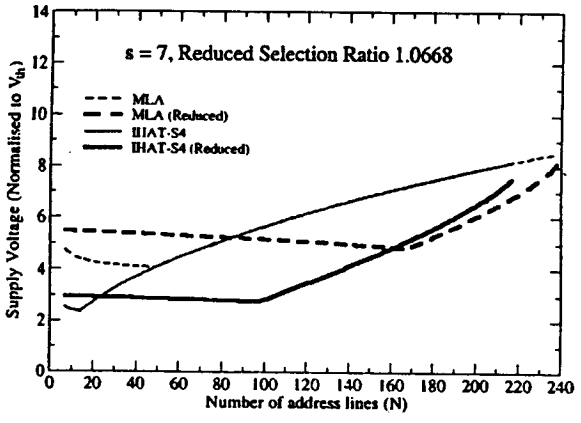

FIGURE 13 — Supply voltage (normalized to V_{th}) *vs.* N for IHAT-S4 and MLA when $s = 7$ and SR = 1.0668.

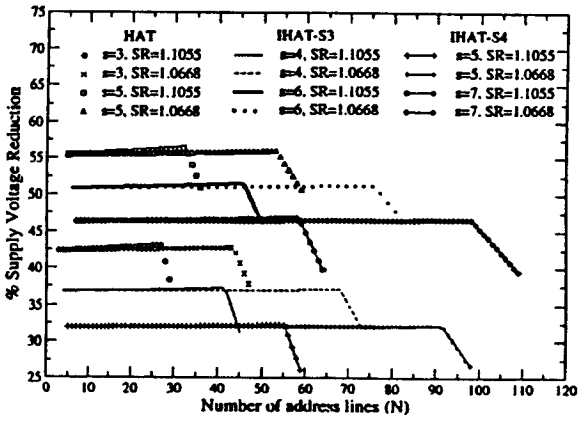

FIGURE 14 — Percentage reduction in supply voltage *vs.* number of address lines (N) in comparison with MLA (Ref. 5).

TABLE 7 — Addressing techniques which have the lowest supply voltage and the range of N over which the supply voltage is low for LC1.

Reduced selection ratio: 1.1055				
Technique	Range of N	Supply voltage (Normalized to V_{th}) V_{sup}	Minimum supply voltage	
			N	V_{sup} (Normalized to V_{th})
APT / IAPT	$3 \le N \le 19$	$2.1002 \le V_{sup} \le 2.0548$	19	2.0548
HAT ($s = 3$)	$3 \le N \le 27$	$2.0975 \le V_{sup} \le 2.0000$	27	2.0000
HAT ($s = 5$)	$5 \le N \le 32$	$2.0851 \le V_{sup} \le 1.9653$	30	1.9761
HAT ($s = 7$)	$7 \le N \le 43$	$2.0802 \le V_{sup} \le 2.3101$	35	1.9428
IHAT-S3 ($s = 6$)	$43 \le N \le 52$	$2.3468 \le V_{sup} \le 2.6896$	42	2.3525
IHAT-S4 ($s = 7$)	$52 \le N \le 87$	$2.7324 \le V_{sup} \le 4.5592$	56	2.7048
MLA ($s = 7$)	$87 \le N \le 100$	$4.6005 \le V_{sup} \le 5.6344$	91	4.4969

TABLE 8 — Addressing techniques which have the lowest supply voltage and the range of N over which the supply voltage is low for LC2.

Reduced selection ratio: 1.0668				
Technique	Range of N	Supply voltage (Normalized to V_{th}) V_{sup}	Minimum supply voltage	
			N	V_{sup} (Normalized to V_{th})
APT / IAPT	$3 \le N \le 30$	$2.0646 \le V_{sup} \le 2.0348$	30	2.0348
HAT ($s = 3$)	$3 \le N \le 43$	$2.0635 \le V_{sup} \le 2.0008$	42	2.0025
HAT ($s = 5$)	$5 \le N \le 53$	$2.0601 \le V_{sup} \le 1.9770$	50	1.9828
HAT ($s = 7$)	$7 \le N \le 72$	$2.0567 \le V_{sup} \le 2.3489$	56	1.9680
IHAT-S3 ($s = 6$)	$72 \le N \le 88$	$2.3692 \le V_{sup} \le 2.7727$	72	2.3692
IHAT-S4 ($s = 7$)	$88 \le N \le 161$	$2.7712 \le V_{sup} \le 4.8306$	98	2.7481
MLA ($s = 7$)	$161 \le N \le 240$	$4.8531 \le V_{sup} \le 8.1275$	168	4.8174

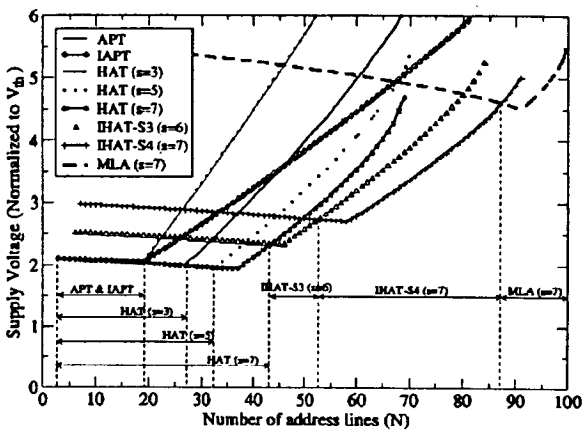

FIGURE 15 — Supply voltage *vs.* *N* for various addressing techniques indicating the range wherein the supply voltage is the lowest for LC1.

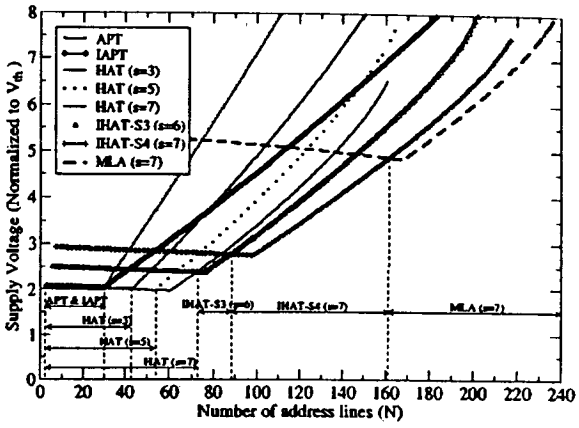

FIGURE 16 — Supply voltage *vs.* *N* for various addressing techniques indicating the range wherein the supply voltage is the lowest for LC2.

matrix corresponding to the Rademacher functions. For example, the Rademacher functions for selecting four rows at a given instant of time have 16 row-select patterns (4 × 16 matrix). This matrix can be interpreted as four orthogonal matrices of 4 × 4. Hence, the large number of row-select patterns just corresponds to using more than one orthogonal matrix or set of functions. This helps in increasing the brightness uniformity of the pixels and decreases the hardware complexity of the column drivers. In summary, the hybrid addressing techniques with lower hardware com-

TABLE 9 — The measured RMS voltages and the percentage of error compared to the theoretical value for different values of *N* and *s* for HAT.

Hybrid addressing technique								
Liquid-crystal material (LC1) : Selection ratio (SR) = 1.1055								
Theoretical : $V_{on} = 1.1055\,V$, $V_{off} = 1.0000\,V$, $V_{th} = 1\,V$								
N	*s*	$V_{sup}(V)$	$V_{on}(V)$	% Error	$V_{off}(V)$	% Error	SR	% Error
18	3	2.04	1.1044	0.0995	0.9995	0.0500	1.1049	0.0543
27	3	2.00	1.1047	0.0724	0.9983	0.1700	1.1065	-0.0905
51	3	4.05	1.1022	0.2985	0.9972	0.2800	1.1053	0.0181
20	5	2.02	1.1025	0.2714	0.9965	0.3500	1.1063	-0.0724
30	5	2.00	1.1055	0.0000	0.9997	0.0300	1.1058	-0.0271
50	5	3.20	1.1051	0.0362	0.9986	0.1400	1.1066	-0.0995
Liquid-crystal material (LC2) : Selection ratio (SR) = 1.0668								
Theoretical : $V_{on} = 1.0668\,V$, $V_{off} = 1.0000\,V$, $V_{th} = 1\,V$								
N	*s*	$V_{sup}(V)$	$V_{on}(V)$	% Error	$V_{off}(V)$	% Error	SR	% Error
18	3	2.04	1.0645	0.2156	0.9986	0.1400	1.0660	0.0750
42	3	2.00	1.0640	0.2625	0.9982	0.1800	1.0659	0.0844
84	3	4.02	1.0625	0.4031	0.9965	0.3500	1.0662	0.0562
126	3	6.38	1.0677	-0.0844	1.0023	-0.2300	1.0652	0.1500
20	5	2.04	1.0661	0.0656	0.9986	0.1400	1.0675	-0.0656
45	5	2.00	1.0663	0.0469	0.9971	0.2900	1.0694	-0.2437
100	5	3.94	1.0681	-0.1219	0.9996	0.0400	1.0685	-0.1594
130	5	5.38	1.0655	0.1219	0.9982	0.1800	1.0674	-0.0562

TABLE 10 — The measured RMS voltages and the percentage of error compared to the theoretical value for different values of N and s for IHAT-S3.

Improved hybrid addressing technique – S3								
Liquid-crystal material (LC1) : Selection ratio (SR) = 1.1055								
Theoretical : $V_{on} = 1.1055\ V$, $V_{off} = 1.0000\ V$, $V_{th} = 1\ V$								
N	s	$V_{sup}(V)$	$V_{on}(V)$	% Error	$V_{off}(V)$	% Error	SR	% Error
20	4	2.58	1.1053	0.0181	0.9990	0.1000	1.1064	-0.0814
40	4	2.50	1.1051	0.0362	0.9986	0.1400	1.1066	-0.0995
60	4	3.75	1.1058	-0.0271	0.9998	0.0200	1.1059	-0.0362
80	4	5.88	1.1050	0.0452	0.9982	0.1800	1.1069	-0.1266
18	6	2.47	1.1044	0.0995	0.9963	0.3700	1.1085	-0.2714
42	6	2.35	1.1051	0.0362	0.9951	0.4900	1.1105	-0.4523
66	6	3.58	1.1058	-0.0271	0.9942	0.5800	1.1122	-0.6061
84	6	5.24	1.1054	0.0090	0.9944	0.5600	1.1116	-0.5518
Liquid-crystal material (LC2) : Selection ratio (SR) = 1.0668								
Theoretical : $V_{on} = 1.0668\ V$, $V_{off} = 1.0000\ V$, $V_{th} = 1\ V$								
N	s	$V_{sup}(V)$	$V_{on}(V)$	% Error	$V_{off}(V)$	% Error	SR	% Error
32	4	2.56	1.0633	0.3281	0.9951	0.4900	1.0685	-0.1594
64	4	2.50	1.0654	0.1312	0.9973	0.2700	1.0683	-0.1406
128	4	4.97	1.0611	0.5343	0.9942	0.5800	1.0673	-0.0469
160	4	6.47	1.0665	0.0281	0.9991	0.0900	1.0675	-0.0656
36	6	2.43	1.0634	0.3187	0.9944	0.5600	1.0694	-0.2437
66	6	2.38	1.0624	0.4124	0.9955	0.4500	1.0672	-0.0375
126	6	4.13	1.0653	0.1406	0.9937	0.6300	1.0721	-0.4968
186	6	6.80	1.0628	0.3750	0.9942	0.5800	1.0690	-0.2062

TABLE 11 — The measured RMS voltages and the percentage of error compared to the theoretical value for different values of N and s for IHAT-S4.

Improved hybrid addressing technique – S4								
Liquid-crystal material (LC1) : Selection ratio (SR) = 1.1055								
Theoretical : $V_{on} = 1.1055\ V$, $V_{off} = 1.0000\ V$, $V_{th} = 1\ V$								
N	s	$V_{sup}(V)$	$V_{on}(V)$	% Error	$V_{off}(V)$	% Error	SR	% Error
25	5	3.09	1.1049	0.0543	0.9974	0.2600	1.1078	-0.2081
55	5	2.92	1.1051	0.0362	0.9963	0.3700	1.1092	-0.3347
85	5	5.00	1.1070	-0.1357	0.9985	0.1500	1.1087	-0.2895
28	7	2.87	1.1026	0.2623	0.9927	0.7300	1.1107	-0.4704
56	7	2.70	1.1012	0.3890	0.9944	0.5600	1.1074	-0.1719
84	7	4.30	1.1024	0.2804	0.9960	0.4000	1.1068	-0.1176
Liquid-crystal material (LC2) : Selection ratio (SR) = 1.0668								
Theoretical : $V_{on} = 1.0668\ V$, $V_{off} = 1.0000\ V$, $V_{th} = 1\ V$								
N	s	$V_{sup}(V)$	$V_{on}(V)$	% Error	$V_{off}(V)$	% Error	SR	% Error
25	5	3.10	1.0650	0.1687	0.9956	0.4400	1.0697	-0.2718
90	5	2.97	1.0604	0.5999	0.9930	0.7000	1.0679	-0.1031
125	5	4.16	1.0586	0.7687	0.9908	0.9200	1.0684	-0.1500
195	5	6.88	1.0608	0.5624	0.9934	0.6600	1.0678	-0.0937
49	7	2.85	1.0594	0.6937	0.9914	0.8600	1.0686	-0.1687
98	7	2.74	1.0600	0.6374	0.9918	0.8200	1.0688	-0.1875
161	7	4.83	1.0598	0.6562	0.9948	0.5200	1.0653	0.1406
189	7	5.94	1.0584	0.7874	0.9930	0.7000	1.0659	0.0844

plexity and reduced supply voltage are a better choice for driving passive-matrix LCDs, especially in portable equipment such as mobile phones and PDAs.

References

1 T N Ruckmongathan and N V Madhusudana, "New addressing techniques for multiplexed liquid crystal displays," *Proc SID* **24**, No. 3, 259-262 (1983).

2 T N Ruckmongathan, "A generalized addressing technique for RMS responding matrix LCDs," *Proc 18th IDRC*, 80-85 (1988).

3 T N Ruckmongathan, "An addressing technique with reduced hardware complexity," *SID Intl Symp Digest Tech Papers*, 65-68 (1994).

4 S Ihara *et al*, "A color STN-LCD with improved contrast, uniformity, and response times," *SID Intl Symp Digest Tech Papers*, 232-235 (1992).

5 K E Kuijk, "Minimum-voltage driving of STN LCDs by optimized multiple row addressing," *Proc EuroDisplay '99*, 77-80 (1999).

6 T N Ruckmongathan, "Novel addressing methods for fast responding LCDs," *Reports Res Lab Asahi Glass Co Ltd* **43** (1), 65-87 (1993).

7 P M Alt and P Pleshko, "Scanning limitations of liquid crystal displays," *IEEE Trans Electron Dev* **ED-21**, 146-155 (1974).

8 H Kawakami *et al*, "Matrix addressing technology of twisted nematic liquid crystal display," *Conf Rec Biennial Display Research Conf*, 50-53 (1976).

9 T J Scheffer and B Clifton, "Active addressing method for high-contrast video-rate STN displays," *SID Intl Symp Digest Tech Papers*, 228-231 (1992).

K. G. Panikumar received his M.Sc degree in electronics from the University of Mysore, Mysore, India, in 1996. He is currently working toward his Ph.D. degree at the Raman Research Institute, Bangalore, India. His research interests are addressing techniques and controllers for passive-matrix LCDs. He is a student member of SID.

T. N. Ruckmongathan's area of research is the addressing of passive-matrix LCDs. He has invented several addressing techniques for driving rms-responding LCDs and ferroelectric LCDs. The Improved Hybrid Addressing Technique he proposed at IDRC '88 was the first of several multi-line addressing techniques that were used in products like PDAs and mobile telephones. He is an associate professor at the Raman Research Institute. In the past, he was a visiting professor at Chalmers University of Technology, Sweden (1998), Guest Researcher at Asahi Glass Co., Japan (1991-93), and an LCD specialist at Philips, The Netherlands (1989-91).

Photograph 3-1: A 64×64 matrix TN LCD displaying four waveforms by selecting 8 rows at a time.

Photograph 3-2: A 64×64 matrix TN LCD displaying four non overlapping waveforms by selecting 8 rows at a time.

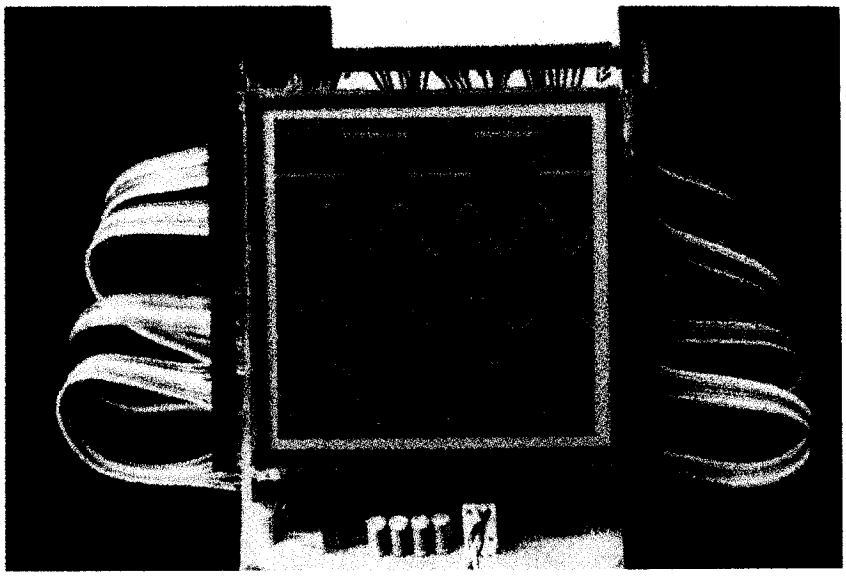

Photograph 3-3: A 64×64 matrix TN LCD displaying four waveforms selecting 16 rows at a time.

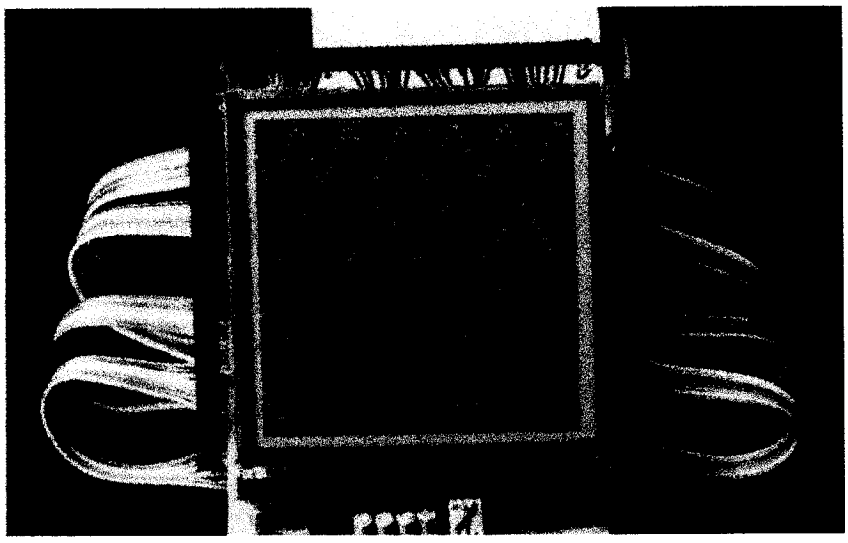

Photograph 3-4: A 64×64 matrix TN LCD displaying four waveforms selecting 16 rows at a time.

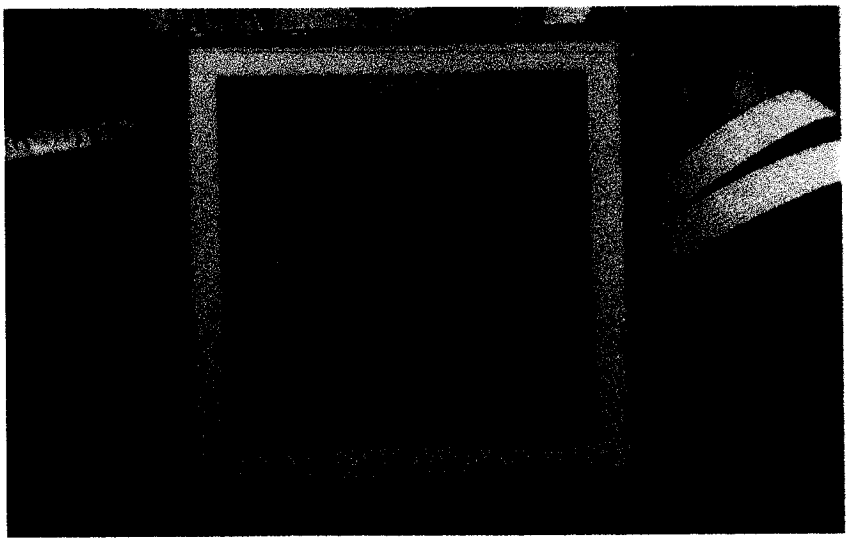

Photograph 4-1: 32×32 matrix LCD displaying 16 gray shades using successive approximation by selecting three rows at a time.

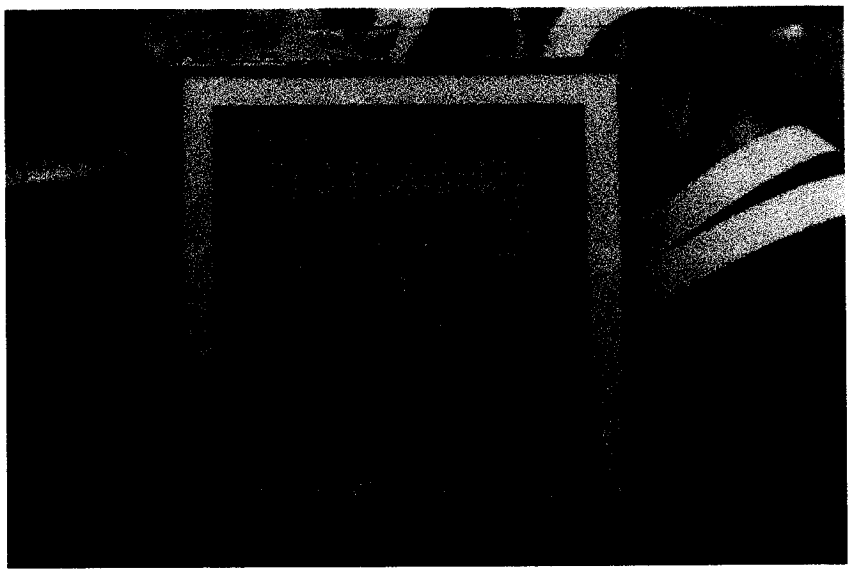

Photograph 4-2: 32×32 matrix LCD displaying 16 gray shades using successive approximation by selecting three rows at a time.